

Spectral function of the Higgs mode in $4 - \varepsilon$ dimensions

Yaniv Tenenbaum Katan and Daniel Podolsky

Physics Department, Technion – Israel Institute of Technology, Haifa 32000, Israel

We investigate the amplitude (Higgs) mode of the relativistic $O(N)$ model in the vicinity of the Wilson-Fisher quantum critical point in $D = 4 - \varepsilon$ spacetime dimensions. We compute the universal part of the scalar spectral function near the transition, to leading non-trivial order in the ordered phase, and to next to leading order in both the disordered phase and the quantum critical regime. We find that, in the disordered phase, the spectral function has a threshold behavior with no Higgs-like peak, whereas in the ordered phase, the Higgs mode appears as a well defined resonance. The pole associated with this resonance is purely real in the $D \rightarrow 3 + 1$ limit, evolving smoothly with dimensionality to become purely imaginary at $D = 2 + 1$ in the $N \rightarrow \infty$ limit. Our results complement previous studies of the scalar spectral function, and demonstrate that the resonance found in these studies can indeed be directly identified with the Higgs mode.

PACS numbers: 74.40.Kb, 67.86.Hj, 11.10.Kk

I. INTRODUCTION

Relativistic field theories with $O(N)$ symmetry describe spontaneous symmetry breaking phase transitions in a large variety of quantum systems. In condensed matter and cold atomic systems, the experimental realizations of these models include, for example, the transverse field Ising model ($N = 1$)^{1–4}, the superfluid to Mott insulator transition ($N = 2$)^{5,6}, and the Néel transition in dimerized antiferromagnets ($N = 3$)^{7,8}.

Breaking of symmetry gives rise to collective modes. When the broken symmetry is continuous, these excitations include massless Goldstone modes, which are related to fluctuations in the direction of the order parameter, and, in systems with emergent relativistic invariance, to a massive Higgs mode associated with fluctuations in the order parameter amplitude^{9,10}.

The Higgs mode and the Goldstone modes are both long lived at the mean field level. However, effects beyond mean field allow for the decay of the Higgs mode into pairs of Goldstone modes. As a result, the Higgs mode acquires a finite lifetime, thus bringing into question its visibility in experiments. This question is especially relevant to systems in $D < 4$ spacetime dimensions, that is, in $d < 3$ spatial dimensions (we consider relativistically invariant quantum critical points, for which $D = d + 1$). In this case the emission of Goldstone modes leads to an infrared divergence in the longitudinal susceptibility^{11–13}, the standard correlation function used to probe the Higgs mode. However, this effect is sensitive to the response function used to probe the mode, and in particular to its symmetry^{14–16}. Specifically, such infrared divergence has been shown to be absent the scalar response function¹⁶. A measurement of this type has been performed on cold bosons in an optical lattice, where the Higgs mode was experimentally observed near the Mott insulator to superfluid transition⁶.

The spacetime dimensionality D also plays an important role in the nature of the ordering transition at the quantum critical point (QCP). For $D = 3 + 1$, the

non-linear coupling decays logarithmically as the QCP is approached and the QCP itself is a Gaussian fixed point^{17,18}. This leads to a Higgs decay width that tends to zero faster than its mass, rendering the Higgs mode “critically-well defined”^{11,19,20}. By contrast, for $2 < D < 4$ the QCP is a Wilson-Fisher fixed point and the interactions remain finite as the Higgs mass approaches zero. In this sense, the interactions are fundamentally strong close to the critical point, and it is therefore interesting to study the nature of the Higgs resonance in this case.

The Higgs mode near the QCP at $D = 3$ has been studied using a variety of methods. In particular, the scalar susceptibility was computed analytically in the large N limit²¹, numerically in Quantum Monte Carlo (QMC) simulations^{22–25}, and through a non-perturbative renormalization group (NPRG) approach²⁶. These methods provide valuable information on the nature of the Higgs mode near the QCP, but each approach has its limitations. The analytic results may be far from experimentally relevant systems, for which $N \leq 3$. Similarly, the QMC and NPRG methods rely on numerical analytic continuation of Matsubara frequency response functions, a procedure that is difficult to control. As a result, some disagreement still exists regarding various properties of the Higgs mode. These include quantitative questions such as the precise value of the mass of the Higgs mode, as well as qualitative questions such as the possible appearance of a Higgs-like resonance in the disordered phase.

In this paper we address these questions following a different approach. We obtain the scalar susceptibility near the Wilson-Fisher fixed point near $D = 3 + 1$ spacetime dimensions, using a $D = 4 - \varepsilon$ calculation that is controlled for small ε . We then study the nature of the Higgs excitation by extracting the universal component of the scalar response function near the QCP. This approach has its own limitations when applied to $D = 2 + 1$; however, it provides valuable information that complements previous approaches.

The main results of our analysis are: (1) In the disordered phase, we find that the scalar spectral function has a threshold behavior without an accompanying

Higgs-like resonance. This contrasts numerical results in $D = 2 + 1$ ²³. (2) In the ordered phase, we find that the scalar spectral function features a sharp Higgs peak and extract its associated pole near the Wilson-Fisher fixed point. Furthermore, in the $N \rightarrow \infty$ limit, we study the position of the pole as a function of space-time dimensionality, and find that it evolves smoothly from a purely real pole at $D = 3 + 1$ to a purely imaginary pole at $D = 2 + 1$. The analytic structure of the scalar spectral function was previously studied in the large N approximation²¹ and by holographic methods²⁷. In particular, in Ref.²¹ it was shown that for large but finite N , the pole at $D = 2 + 1$ picks up a small real component. Our results show that this pole is indeed smoothly connected to the sharp Higgs peak at $D = 3 + 1$. (3) In the quantum critical regime, we find that the universal scaling function has a peak at finite frequencies near $D = 3 + 1$. This peak disappears as one approaches $D = 2 + 1$.

This article is organized as follows. In Sec. II we briefly review the $O(N)$ model, the physical observables studied in this work, and their expected scaling near the QCP. In Sec. III we focus on the disordered phase; we calculate the single particle gap, the scalar susceptibility, extract the universal scaling function to next to leading order in ε , and discuss its properties. In Sec. IV we extend the analysis to the ordered phase, and evaluate the scalar susceptibility and its universal scaling function to the first non-trivial order in ε . In addition, we evaluate the scalar response function for $N = \infty$ and general D . In Sec. V we compute the universal scaling function in the quantum critical regime, to next to leading order. In Sec. VI we provide a summary and conclusions. In Appendix A we present the detailed calculations in the ordered phase. In Appendix B we compute the polarization bubble in the quantum critical regime.

II. GENERAL FORMALISM

A. Model

We study the partition function defined by the path integral

$$\mathcal{Z} = \int \mathcal{D}\phi_\alpha \exp(-S[\phi]) \quad (1)$$

$$S[\phi] = \int_x \left[\frac{1}{2} (\partial_\mu \phi_\alpha(x))^2 + \frac{r}{2} \phi_\alpha^2(x) + \frac{U}{8} (\phi_\alpha^2(x))^2 \right]. \quad (2)$$

Here, ϕ_α is a real field with N components, $\alpha \in \{1 \dots N\}$. The action is defined on Euclidean space-time with $\int_x = \int d^D x$ where D is the space-time dimension. The action in Eq. (2) has relativistic invariance, in which the coordinates have been scaled such that the speed of sound is one.

The system described by Eq. (1) undergoes a quantum phase transition at a critical value r_c ^{18,28,29}. For $r > r_c$,

the system is in a disordered phase with $\langle \phi \rangle = 0$. In this phase the $O(N)$ symmetry is preserved and there are N degenerate gapped modes. By contrast, for $r < r_c$ the system is in an ordered phase and the ϕ field acquires an expectation value (EV), $\langle \phi \rangle = (\phi_0, 0, \dots)$ which breaks the $O(N)$ symmetry down to $O(N-1)$.

The breaking of the $O(N)$ symmetry leads to the emergence of collective modes which correspond to fluctuations of the order parameter,

$$\phi = (\phi_0 + \sigma, \vec{\pi}) \quad (3)$$

where the $N-1$ component field $\vec{\pi}$ corresponds to the $N-1$ gapless Goldstone modes and the scalar field σ is associated with the Higgs mode.

B. Physical Observables

The two-point tensor dynamical correlation function of the ϕ_α field is defined by,

$$\chi_{\alpha\beta}(p) = \int_x e^{-i\mathbf{p}\cdot\mathbf{x}} [\langle \phi_\alpha(x) \phi_\beta(0) \rangle - \langle \phi_\alpha(x) \rangle \langle \phi_\beta(0) \rangle]. \quad (4)$$

In the ordered phase, the amplitude fluctuations of the order parameter can be probed by the longitudinal susceptibility,

$$\chi_{11}(p) = \int_x e^{-i\mathbf{p}\cdot\mathbf{x}} [\langle \sigma(x) \sigma(0) \rangle - \langle \sigma(x) \rangle \langle \sigma(0) \rangle] \quad (5)$$

which is the two-point correlation function of the σ field.

Within the mean field approximation, Eq. (5) has a pole corresponding to a gapped excitation¹¹, identified as the Higgs mode. However beyond mean field level, the peak of the Higgs mode broadens as a result of the decay of the Higgs into pairs of Goldstone modes. In particular, for $D < 4$, the longitudinal susceptibility has divergent spectral weight at low frequencies, which overwhelms the Higgs resonance close to the critical point^{11,12}.

We will focus instead on a second observable, the scalar susceptibility, which is the two-point correlation function of the amplitude squared of the field ϕ ,

$$\chi_s(p) = \int_x e^{-i\mathbf{p}\cdot\mathbf{x}} [\langle \phi_\alpha^2(x) \phi_\beta^2(0) \rangle - \langle \phi_\alpha^2(x) \rangle \langle \phi_\beta^2(0) \rangle]. \quad (6)$$

It has been argued¹⁶ that the scalar susceptibility is less sensitive to the emission of Goldstone modes, and therefore produces a sharper resonance for the Higgs mass.

We are interested in the dynamical scalar structure factor function $S(\omega)$, obtained by analytic continuation of the scalar susceptibility,

$$S(\omega) = \Im \{ \chi_s(p \rightarrow -i\omega + 0^+) \} \quad (7)$$

Equation (7) corresponds to zero momentum and a finite probe frequency ω .

C. The Wilson-Fisher Fixed Point

The modern description of critical behavior is based on the assumption that near phase transitions, the long distance properties of a system are determined by the large correlation length ξ , which is the only important length scale^{30,31}. In particular, the critical behavior is dominated by fluctuations that are self similar up to the scale of the correlation length ξ . This last property can be used to build a description of the critical behavior through the Renormalization Group (RG). The RG procedure consists of gradually eliminating the correlated degrees of freedom at length scales $x \ll \xi$, until only uncorrelated, simple degrees of freedom remain at the length scale ξ . In this process, different fixed points of the RG procedure correspond to either phases or to phase transitions.

Applying the RG procedure to Eq. (1) yields that at $D = 4 - \varepsilon$ space time dimensions, this system undergoes a phase transition described by the Wilson-Fisher fixed point^{17,18,28,29}. This result is derived for $D = 4 - \varepsilon$ space time dimensions, but it is generally believed that the fixed point can be smoothly evolved to describe the phase transition in the range $2 < D < 4$.

For $D = 4 - \varepsilon$, the interaction coupling U at the Wilson-Fisher fixed point is of $\mathcal{O}(\varepsilon)$. To $\mathcal{O}(\varepsilon^2)$,²⁸

$$U_c = \frac{2\varepsilon}{N+8} \frac{1}{\Omega_\varepsilon} \left(1 + \frac{9N+42}{(N+8)^2} \varepsilon \right) \quad (8)$$

where $\Omega_\varepsilon = \Lambda^{-\varepsilon} K_{4-\varepsilon}$, $K_D = \frac{2^{1-D} \pi^{-D/2}}{\Gamma(\frac{D}{2})}$ is the normalized area of a D -dimensional sphere, Λ is the implicit ultraviolet cutoff, and Γ is Euler's Gamma function. This allows for a controlled expansion of the physical observables in powers of ε .

In the case of the Wilson-Fisher point, deviations of U away from U_c are irrelevant and flow only slowly to zero. Therefore, in order to extract universal properties near the critical point, we will set $U = U_c$ and use $\delta r = r - r_c$ as the tuning parameter across the transition^{18,28,29}.

D. Scaling

We proceed to obtain the scaling limit²¹ of the dynamical scalar structure factor $S(\omega)$ near the phase transition, in terms of the critical exponents. These critical exponents can be obtained from the RG procedure at the Wilson-Fisher fixed point. We start by deriving the free energy density of Eq. (1), $f = -\frac{1}{V} \ln Z$, with respect to r ,

$$\frac{\partial^2 f}{\partial r^2} = \frac{1}{4V} \int_{x,y} \left[\langle \phi_\alpha^2(x) \phi_\beta^2(y) \rangle - \langle \phi_\alpha^2(x) \rangle \langle \phi_\beta^2(y) \rangle \right] - \frac{1}{U} \quad (9)$$

which is the scalar susceptibility for $p = 0$, up to additive and multiplicative constants. f can be written as a sum of regular and singular parts, where according to

the hyperscaling hypothesis the latter scales as ξ^{-D} . The correlation length, ξ satisfies $\xi \propto |r - r_c|^{-\nu}$, where ν is the correlation length exponent. It follows that

$$S(\omega = 0) \propto \xi^{-D+2/\nu} + \text{regular part}. \quad (10)$$

For a relativistic theory, $\xi \propto \frac{1}{\Delta}$ where Δ is the energy gap of single particle excitations in the disordered phase. Δ serves as a characteristic energy scale at the ordered phase. We conclude that

$$S(\omega) = \mathcal{A}_\pm \Delta^{2\alpha} \Phi_\pm \left(\frac{\omega}{\Delta} \right) + \text{regular part} \quad (11)$$

where $2\alpha = D - \frac{2}{\nu}$. The regular part is non-universal and is analytic in δr , and Φ_\pm are universal scaling functions which describe the critical behavior of $S(\omega)$ in the disordered (Φ_+) and ordered (Φ_-) phases.

In order to fix the overall amplitudes \mathcal{A}_\pm , we look at the asymptotic behavior of $S(\omega)$ in different regimes. In the disordered phase, we find that $S(\omega)$ has a threshold at $\omega = 2\Delta$. Near the threshold,

$$S(\omega) \sim \mathcal{A}_+ \Delta^{2\alpha} \left(\frac{\delta\omega}{\Delta} \right)^{(D-3)/2} \Theta(\delta\omega), \quad (12)$$

where $\delta\omega \equiv \omega - 2\Delta$ and where $\Theta(x)$ is the Heaviside step function. On the other hand, in the ordered phase and at low frequencies $0 < \omega \ll \Delta$, we find

$$S(\omega) \sim \mathcal{A}_- \Delta^{2\alpha} \left(\frac{\omega}{\Delta} \right)^D. \quad (13)$$

We will use these asymptotic forms to define \mathcal{A}_\pm . Their individual values are not universal (*e.g.* they depend on the UV cutoff), but their ratio is. We find,

$$\frac{\mathcal{A}_+}{\mathcal{A}_-} = \frac{4N}{N-1} \quad (14)$$

Note that the definition for \mathcal{A}_+ is slightly different from that used in Ref.²¹, where the logarithmic threshold singularity, specific to $D = 2 + 1$, was used. Hence, a straightforward comparison of the ratio obtained in both approaches is not possible.

At $T > 0$, the temperature serves as a second characteristic energy scale. In particular, at $r = r_c$, the scaling of $S(\omega)$ at finite temperatures becomes

$$S(\omega) = \mathcal{A}_T T^{2\alpha} \Phi_T \left(\frac{\omega}{T} \right) + \text{regular part} \quad (15)$$

where Φ_T is the thermal universal scaling function.

We will compute the universal scaling functions Φ_\pm and Φ_T near the Wilson-Fisher fixed point.

III. THE DISORDERED PHASE

In this section we focus on the disordered phase ($\delta r > 0$) at $T = 0$, in which the $O(N)$ symmetry is preserved. We extract the single-particle gap Δ from the poles of the longitudinal susceptibility, obtain the universal part of the scalar susceptibility $\Phi_+(\frac{\omega}{\Delta})$, and study the threshold singularity of this physical observable.

A. Critical Point

We begin by determining the value of r at the transition, by requiring²¹ $G(0, r_c)^{-1} = 0$, where $G(p, r) = \chi_{\alpha\alpha}(p, r)$ is the two point correlation function of the ϕ_α field in the disordered phase.

We obtain r_c for $D = 4 - \varepsilon$ at $U = U_c$, as given in Eq. (8). The Dyson expansion for $G(p, r)$ to $\mathcal{O}(\varepsilon^2)$ yields

$$G^{-1}(p, r) = p^2 + r + \frac{U_c(N+2)}{2} \int_q \frac{1}{q^2 + r - \Sigma_1(r)} - \frac{U_c^2(N+2)}{2} \int_q \frac{\Pi(q, \sqrt{r})}{(\mathbf{p} + \mathbf{q})^2 + r} \quad (16)$$

where $\int_q \equiv \int \frac{d^{4-\varepsilon}q}{(2\pi)^{4-\varepsilon}}$. Here, $\Pi(q, \sqrt{r})$ is the polarization bubble,

$$\Pi(q, \sqrt{r}) = \int_k \frac{1}{((\mathbf{q} + \mathbf{k})^2 + r)(k^2 + r)}, \quad (17)$$

and

$$\Sigma_1(r) = -\frac{U_c(N+2)}{2} \int_q \frac{1}{q^2 + r}. \quad (18)$$

The equation for r_c is then

$$0 = r_c + \frac{U_c(N+2)}{2} \int_q \frac{1}{q^2 + r_c - \Sigma_1(r_c)} - \frac{U_c^2(N+2)}{2} \int_q \frac{\Pi(q, \sqrt{r_c})}{q^2 + r_c}. \quad (19)$$

From inspection of Eqs. (18) and (19), we conclude that $r_c = \Sigma_1(r_c) + \mathcal{O}(\varepsilon^2)$. We can use this to write Eq. (19) to $\mathcal{O}(\varepsilon^2)$ as

$$r_c = -\frac{U_c(N+2)}{2} \left(\int_q \frac{1}{q^2} - U_c \int_q \frac{\Pi(q, 0)}{q^2} \right). \quad (20)$$

By performing the integrals in Eq. (20), we find

$$r_c = \frac{U_c(N+2)K_D}{2} \frac{\Lambda^{D-2}}{2-D} \left(1 - \frac{U_c K_D \Lambda^{D-4}}{D-3} \right) \quad (21)$$

Hence, using Eq. (8), we obtain

$$r_c = -\varepsilon \frac{\Lambda^{2-2\varepsilon}}{2} \frac{N+2}{N+8} \left(1 - \varepsilon \frac{N^2 + 30N + 116}{2(N+8)^2} \right) + \mathcal{O}(\varepsilon^3). \quad (22)$$

In what follows we write

$$r = r_c + \delta r \quad (23)$$

such that the quantum phase transition occurs at $\delta r = 0$.

B. Single Particle Gap

The single particle gap Δ is determined by the condition²¹ $G(p = -i\Delta, \delta r)^{-1} = 0$. Using Eqs. (18) and (22), Eq. (16) becomes

$$G^{-1}(p, \delta r) = p^2 + \delta r + \frac{U_c(N+2)}{2} \times \left(\int_q \frac{1}{q^2 + \delta r} - \int_q \frac{1}{q^2} \right) + \mathcal{O}(\varepsilon^2).$$

It follows that the pole of $G(p, \delta r)$ is at $p^2 = -\Delta^2$, where

$$\begin{aligned} \Delta^2 &= \delta r \left(1 - \frac{\varepsilon}{2} \frac{N+2}{N+8} \ln \frac{\Lambda^2}{\delta r} \right) + \mathcal{O}(\varepsilon^2) \\ &= \Lambda^2 \left(\frac{\delta r}{\Lambda^2} \right)^{2\nu} + \mathcal{O}(\varepsilon^2), \end{aligned} \quad (24)$$

and $\nu = \frac{1}{2} + \frac{\varepsilon}{4} \frac{N+2}{N+8}$. Equation (24) provides the required relation between the energy gap Δ and the tuning parameter δr ^{11,17,18,21,32}. Note that to this order in ε , the renormalized propagator is simply

$$G(p, \delta r) = \frac{1}{p^2 + \Delta^2} + \mathcal{O}(\varepsilon^2) \quad (25)$$

where Δ is related to δr by Eq. (24).

C. Scalar Susceptibility

The scalar susceptibility can be evaluated order by order in ε . The diagrammatic expansion of this calculation is given to $\mathcal{O}(\varepsilon)$ in Fig. 1. We find

$$\chi_s(p, \delta r) = 2N\Pi(p, \Delta) - U_c N(N+2)\Pi(p, \Delta)^2 + \mathcal{O}(\varepsilon^2). \quad (26)$$

Here, $\Pi(p, \Delta)$ is the polarization bubble, Eq. (17), which evaluates to

$$\begin{aligned} \Pi(p, \Delta) &= \Omega_\varepsilon \left[\frac{1}{2} - \frac{\tanh^{-1} x}{x} + \frac{1}{2} \ln \frac{\Lambda^2}{\Delta^2} \right. \\ &\quad + \varepsilon \left\{ \frac{1}{4x} \left(\text{Li}_2 \left(\frac{1+x}{2} \right) - \text{Li}_2 \left(\frac{1-x}{2} \right) \right) \right. \\ &\quad \left. - \frac{\tanh^{-1} x}{2x} \left(1 - \frac{1}{2} \ln \frac{p^2}{x^2 \Delta^2} - \ln \frac{\Lambda^2}{\Delta^2} \right) \right. \\ &\quad \left. \left. + \frac{3}{8} + \frac{\pi^2}{6} + \frac{1}{8} \left(1 + \ln \frac{\Lambda^2}{\Delta^2} \right)^2 \right\} \right] + \mathcal{O}(\varepsilon^2), \end{aligned} \quad (27)$$

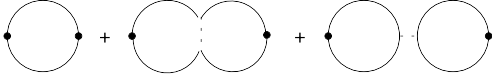


Figure 1: The diagrams which contribute to the scalar susceptibility in the disordered phase, to first non-trivial order. The solid lines are renormalized propagators, Eq. (25).

where $x = \frac{p}{\sqrt{p^2 + 4\Delta^2}}$ and $\text{Li}_2(z)$ is the dilogarithm function, defined by $\text{Li}_2(z) = -\int_0^z \frac{\ln(1-t)}{t} dt$.

The explicit expression for the scalar susceptibility is obtained by inserting Eq. (27) and Eq. (8) into Eq. (26),

$$\begin{aligned} \frac{\Omega_\varepsilon^{-1}}{N} \chi_s(p, \delta r) = & 1 + \ln \frac{\Lambda^2}{\Delta^2} - \frac{\alpha_1 \varepsilon}{2} \left(1 + \ln \frac{\Lambda^2}{\Delta^2} \right)^2 + \frac{\alpha_1 \varepsilon}{2} \\ & - \frac{2 \tanh^{-1} x}{x} \left[1 - \alpha_1 \varepsilon \left(1 + \ln \frac{\Lambda^2}{\Delta^2} \right) \right] \\ & + \varepsilon \chi_2(p) + \mathcal{O}(\varepsilon^2) \end{aligned} \quad (28)$$

where

$$\begin{aligned} \chi_2(p) = & \frac{\pi^2}{12} + \frac{\tanh^{-1} x}{2x} \ln \frac{p^2}{x^2 \Delta^2} - 2 \frac{N+2}{N+8} \left(\frac{\tanh^{-1} x}{x} \right)^2 \\ & + \frac{1}{2x} \left[\text{Li}_2 \left(\frac{1-x}{2} \right) - \text{Li}_2 \left(\frac{1+x}{2} \right) \right] + \frac{1}{2} \frac{N+14}{N+8}, \end{aligned}$$

and α_1 is given in Eq. (31) below.

D. Universal Scaling Function

As argued in Sec. IID, near the transition, the scalar susceptibility takes the form,

$$\chi_s(p, \delta r) = \mathcal{A}_+ \Delta^{2\alpha} \tilde{\Phi}_+ \left(\frac{p}{\Delta} \right) + \text{regular part} \quad (29)$$

where $2\alpha = D - 2/\nu$. To $\mathcal{O}(\varepsilon^2)$, the critical exponent α is given by²⁸

$$\alpha = \alpha_1 \varepsilon + \alpha_2 \varepsilon^2 + \mathcal{O}(\varepsilon^3), \quad (30)$$

where,

$$\begin{aligned} \alpha_1 &= \frac{1}{2} \frac{N-4}{N+8}, \\ \alpha_2 &= \frac{(N+2)(13N+44)}{2(N+8)^3}. \end{aligned} \quad (31)$$

$\tilde{\Phi}_+ \left(\frac{\omega}{\Delta} \right)$ is related to the universal scaling function $\Phi_+ \left(\frac{\omega}{\Delta} \right)$ by a Wick rotation,

$$\Phi_+ \left(\frac{\omega}{\Delta} \right) = \Im \left\{ \tilde{\Phi}_+ \left(-\frac{i\omega}{\Delta} + 0^+ \right) \right\}. \quad (32)$$

We evaluate $\tilde{\Phi}_+ \left(\frac{\omega}{\Delta} \right)$, the universal component of Eq. (28). We choose

$$\mathcal{A}_+ = \Omega_\varepsilon \Lambda^{-2\alpha} N \pi (1 - \varepsilon \alpha_1 - \frac{\varepsilon}{2} \ln 2). \quad (33)$$

which gives the normalization in Eq. (12), as will be shown later. Then, we can expand $\tilde{\Phi}_+ \left(\frac{p}{\Delta} \right)$ in non-negative powers of ε as $\tilde{\Phi}_+ \left(\frac{p}{\Delta} \right) = \tilde{\Phi}_0 + \varepsilon \tilde{\Phi}_1 + \varepsilon^2 \tilde{\Phi}_2 + \mathcal{O}(\varepsilon^3)$ and write

$$\begin{aligned} \mathcal{A}_+ \Delta^{2\alpha} \tilde{\Phi}_+ &= \frac{\tilde{\Phi}_0}{\varepsilon} + \tilde{\Phi}_1 - \alpha_1 \tilde{\Phi}_0 \lambda + \varepsilon \tilde{\Phi}_2 \\ &\quad - \left(\alpha_2 \tilde{\Phi}_0 + \alpha_1 \tilde{\Phi}_1 \right) \varepsilon \lambda \\ &\quad + \frac{1}{2} \alpha_1^2 \tilde{\Phi}_0 \varepsilon \lambda^2 + \mathcal{O}(\varepsilon^2) \end{aligned} \quad (34)$$

where $\lambda \equiv \ln \frac{\Lambda^2}{\Delta^2}$. We can now obtain $\tilde{\Phi}_0$, $\tilde{\Phi}_1$ and $\tilde{\Phi}_2$ by comparing Eqs. (28) and (34) order by order in both ε and λ . Indeed, we find that the scalar susceptibility is of the scaling form, Eq. (29), with

$$\begin{aligned} \tilde{\Phi}_+ \left(\frac{p}{\Delta} \right) &= -\frac{2}{\pi} (1 - \alpha_1 \varepsilon) \frac{\tanh^{-1} x}{x} \\ &\quad + \frac{\varepsilon}{\pi} \chi_2(p) - \mathcal{C} + \mathcal{O}(\varepsilon^2) \end{aligned} \quad (35)$$

where $\mathcal{C} = \frac{1}{\alpha_1 \pi} \left(\frac{1}{\varepsilon} - \alpha_1 - \frac{\alpha_2}{\alpha_1} \right)$ is a real constant which does not contribute to the real frequency function Φ_+ . In addition, we find that the non-universal part in Eq. (29) is given by the constant

$$\chi_{reg} = N \Omega_\varepsilon \left(\frac{1}{\alpha_1 \varepsilon} - \frac{\alpha_2}{\alpha_1^2} \right). \quad (36)$$

As a consistency check, we examine the asymptotic behavior of Eq. (35) in the limit $p \gg \Delta$. In this limit, the universal component is expected to take the form²¹

$$\tilde{\Phi}_+ \left(\frac{p}{\Delta} \right) \propto \left(\frac{p}{\Delta} \right)^{2\alpha} \quad (37)$$

In the same limit, Eq. (35) becomes

$$\begin{aligned} \tilde{\Phi}_+ \left(\frac{p}{\Delta} \right) &\rightarrow -\mathcal{C} - \frac{2}{\pi} (1 - \alpha_1 \varepsilon) \ln \frac{p}{\Delta} + \frac{\varepsilon}{2\pi} \frac{N+14}{N+8} \\ &\quad - \frac{2}{\pi} \alpha_1 \varepsilon \ln^2 \frac{p}{\Delta} + \mathcal{O} \left(\frac{\Delta}{p} \right) + \mathcal{O}(\varepsilon^2) \\ &= -\mathcal{C} \left(\frac{p}{\Delta} \right)^{2\alpha} + \varepsilon \frac{1}{2\pi} \frac{N+14}{N+8} \\ &\quad + \mathcal{O} \left(\frac{\Delta}{p} \right) + \mathcal{O}(\varepsilon^2), \end{aligned} \quad (38)$$

as expected. Here, we've used the relation $x^y = 1 + y \ln x + (y \ln x)^2/2 + \mathcal{O}(y^3)$. Note that for $N = 4$, the final expression is not well defined since $\mathcal{C} = \infty$. This is an artifact of our working order in ε since, for $N = 4$, α vanishes to $\mathcal{O}(\varepsilon)$, and hence it is not possible to exponentiate the expression in the top line.

The universal scaling function in the disordered phase can now be obtained by analytic continuation,

$$\begin{aligned} \Phi_+ \left(\frac{\omega}{\Delta} \right) &= \Theta(|\omega| - 2\Delta) \frac{\sqrt{\omega^2 - 4\Delta^2}}{\omega} \times \\ &\quad \left(1 + \varepsilon \Phi_2 \left(\frac{\omega}{\Delta} \right) \right) + \mathcal{O}(\varepsilon^2), \end{aligned} \quad (39)$$

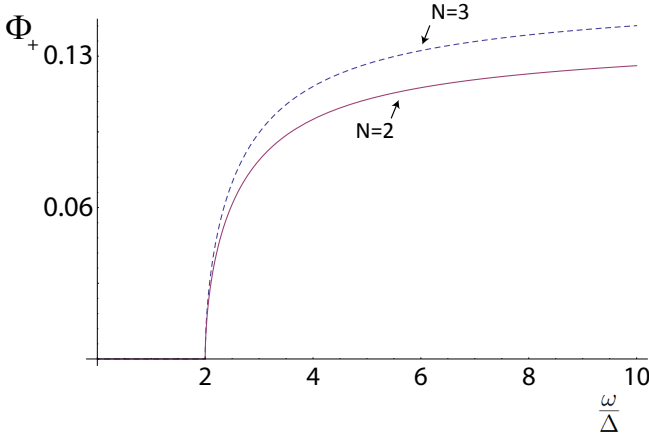


Figure 2: The universal scaling function in the disordered phase, $\Phi_+(\frac{\omega}{\Delta})$, to second order in ε . Results are for $\varepsilon = 0.1$ and for $N = 2, 3$. We find that to this order, the shape of the universal scaling function has very little dependence on ε .

where

$$\begin{aligned} \Phi_2\left(\frac{\omega}{\Delta}\right) = & \frac{1}{2} \ln \left(\frac{2\Delta + \frac{2|\omega|}{\sqrt{\omega^2 - 4\Delta^2}}}{\sqrt{\omega^2 - 4\Delta^2} - |\omega|} \right) \\ & + 2 \frac{N+2}{N+8} \frac{\sqrt{\omega^2 - 4\Delta^2}}{|\omega|} \tanh^{-1} \frac{|\omega|}{\sqrt{\omega^2 - 4\Delta^2}} \\ & + \frac{i}{2\pi} \text{Li}_2 \left(\frac{1}{2} + \frac{|\omega|}{2\sqrt{\omega^2 - 4\Delta^2}} \right) \\ & - \frac{i}{2\pi} \text{Li}_2 \left(\frac{1}{2} - \frac{|\omega|}{2\sqrt{\omega^2 - 4\Delta^2}} \right). \end{aligned} \quad (40)$$

$\Phi_+(\frac{\omega}{\Delta})$ is depicted in Fig. 2. We find that $\Phi_+(\frac{\omega}{\Delta})$ has a threshold at $\omega = 2\Delta$, the minimal energy required to excite a pair of quasiparticles with mass Δ . To first order in ε , $\Phi_+(\frac{\omega}{\Delta})$ does not have a resonance, unlike results obtained in $D = 2 + 1$ using Quantum Monte Carlo²³.

We examine $\Phi_+(\frac{\omega}{\Delta})$ near the threshold, at $\omega = 2\Delta + \delta\omega$ as $\delta\omega \rightarrow 0^+$. We find

$$\begin{aligned} \Phi_+\left(\frac{\delta\omega + 2\Delta}{\Delta}\right) & \sim \Theta(\delta\omega) \sqrt{\frac{\delta\omega}{\Delta}} \left[1 - \frac{\varepsilon}{2} \ln \frac{\delta\omega}{\Delta} \right] \\ & = \Theta(\delta\omega) \left(\frac{\delta\omega}{\Delta} \right)^{(1-\varepsilon)/2} + \mathcal{O}(\varepsilon^2), \end{aligned} \quad (41)$$

which agrees with Eq. (12), hence justifying the choice of \mathcal{A}_+ in Eq. (33). This power law matches the expected behavior based on the density of states available for exciting two counterpropagating bosons with total energy of $\omega = 2\Delta + \delta\omega$,

$$\int \frac{d^{D-1}k}{(2\pi)^{D-1}} \delta\left(\omega - 2\sqrt{k^2 + \Delta^2}\right) \propto \delta\omega^{(D-3)/2} \Theta(\delta\omega). \quad (42)$$

IV. THE ORDERED PHASE

We write the expectation value (EV) of the order parameter in the ordered phase as

$$\langle \phi^2 \rangle = \frac{m^2}{U}, \quad (43)$$

where $m^2 = -2r + \mathcal{O}(\varepsilon)$. We parametrize the fluctuations around the EV as,

$$\phi = \left(\frac{m}{\sqrt{U}} + \sigma, \vec{\pi} \right). \quad (44)$$

In Eq. (44), the fields σ and π represent the longitudinal (Higgs) and transverse (Goldstone) excitations relative to the ordering direction, correspondingly.

The partition function in the ordered phase is obtained by inserting Eq. (44) into Eq. (1),

$$\mathcal{Z} = \int \mathcal{D}\sigma \mathcal{D}\pi \exp(-S_0 - S_C - S_I) \quad (45)$$

where

$$\begin{aligned} S_0 &= \frac{1}{2} \int_x \left[(\partial_\mu \pi)^2 + (\partial_\mu \sigma)^2 + m^2 \sigma^2 \right], \\ S_C &= \frac{m^2 + 2r}{4U} \int_x \left[U \pi^2 + U \sigma^2 + 2m\sqrt{U}\sigma \right], \\ S_I &= \int_x \left[\frac{1}{2} m\sqrt{U} \sigma \pi^2 + \frac{1}{3!} 3m\sqrt{U} \sigma^3 + \right. \\ & \quad \left. \frac{1}{4!} 3U \sigma^4 + \frac{1}{8} U (\pi^2)^2 + \frac{1}{4} U \pi^2 \sigma^2 \right]. \end{aligned} \quad (46)$$

The terms S_0 and S_I are the harmonic and interacting parts of the action, respectively. The resulting tree-level Green's functions are,

$$\begin{aligned} G_{\sigma\sigma}^0(p) &= \frac{1}{p^2 + m^2}, \\ G_{\pi\pi}^0(p) &= \frac{1}{p^2}. \end{aligned} \quad (47)$$

The term S_C contains the counterterms. In principle, three separate counterterms are necessary, one each for the terms π^2, σ^2 , and σ . However, to $\mathcal{O}(\varepsilon)$, all three are fixed by the requirement $\langle \sigma \rangle = 0$. At this order, this single condition guarantees that the Goldstone modes are gapless and that the tree-level mass of the σ field is m .

The condition $\langle \sigma \rangle = 0$ yields, at U_c

$$\begin{aligned} m^2 &= -2r - U_c(N-1) \int_p \frac{1}{p^2} - 3U_c \int_p \frac{1}{p^2 + m^2} + \mathcal{O}(\varepsilon^2) \\ &= -2\delta r + \frac{3m^2}{2(N+8)} \varepsilon \ln \frac{\Lambda^2}{m^2} + \mathcal{O}(\varepsilon^2). \end{aligned} \quad (48)$$

In Eq. (48), we have used the values of r_c , see Eqs. (20). m can be related to the value of the gap in the partner point in the symmetric phase through Eq. (24) as

$$m^2 = 2\Delta^2 \left(1 + \frac{\varepsilon}{2} \ln \frac{\Lambda^2}{2\Delta^2} + \frac{\varepsilon}{2} \frac{N+2}{N+8} \ln 2 \right) + \mathcal{O}(\varepsilon^2). \quad (49)$$

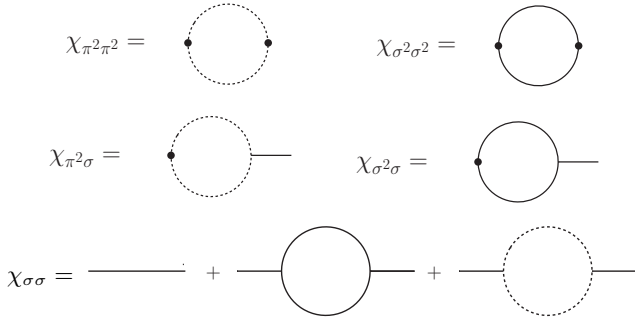


Figure 3: Diagrammatic expansion of the scalar susceptibility χ_s to $\mathcal{O}(\varepsilon^0)$, written in terms of the susceptibilities that compose it in the ordered phase. $\chi_{\pi^2\pi^2}$ and $\chi_{\sigma^2\sigma^2}$ are calculated to $\mathcal{O}(\varepsilon^0)$, $\chi_{\sigma^2\sigma}$ and $\chi_{\pi^2\sigma}$ to $\mathcal{O}(\varepsilon^{1/2})$ and $\chi_{\sigma\sigma}$ to $\mathcal{O}(\varepsilon)$. At this order, $\chi_{\pi^2\sigma^2} = 0$.

This indicates that m^2 and Δ^2 scale with different exponents. This is expected. Despite the fact that m^2 has units of mass squared, Eq. (43) shows that it scales with the order parameter exponent β , rather than ν .

A. Scalar Susceptibility

In order to compute the scalar susceptibility in the ordered phase, we use Eq. (44) to obtain, at U_c ,

$$\phi_\alpha^2(x) = \pi^2 + \sigma^2 + 2\sigma \frac{m}{\sqrt{U_c}} + \frac{m^2}{U_c}. \quad (50)$$

Inserting this into Eq. (6) yields,

$$\begin{aligned} \chi_s(p) &= \chi_{\pi^2\pi^2} + \chi_{\sigma^2\sigma^2} + 2\chi_{\pi^2\sigma^2} \\ &\quad + 4 \frac{m}{\sqrt{U_c}} (\chi_{\pi^2\sigma} + \chi_{\sigma^2\sigma}) + 4 \frac{m^2}{U_c} \chi_{\sigma\sigma}. \end{aligned} \quad (51)$$

We evaluate $\chi_s(p)$ by summing over the different susceptibilities in Eq. (51). Since $U_c = \mathcal{O}(\varepsilon)$, the leading term in χ_s is of $\mathcal{O}(\varepsilon^{-1})$. Here we compute the scalar susceptibility to the next-to-leading order, $\mathcal{O}(\varepsilon^0)$. This yields the diagrams shown in Fig. 3, which evaluate to,

$$\begin{aligned} \Omega_\varepsilon^{-1} \chi_s &= \frac{1}{\varepsilon} \frac{2m^2(N+8)}{p^2+m^2} + \frac{(N-1)p^4}{(p^2+m^2)^2} \left(1 + \ln \frac{\Lambda^2}{p^2}\right) \\ &\quad + \frac{(p^2-2m^2)^2}{(p^2+m^2)^2} \left(1 + \ln \frac{\Lambda^2}{m^2} - \frac{2 \tanh^{-1} x_m}{x_m}\right), \end{aligned} \quad (52)$$

where $x_m = \frac{p}{\sqrt{p^2+4m^2}}$. The calculation of $\chi_s(p)$ to $\mathcal{O}(\varepsilon)$ is outlined in App. A.

B. Universal Scaling Function

Near the phase transition, Eq. (52) can be written in the form

$$\chi_s(p) = \mathcal{A}_- \Delta^{2\alpha} \tilde{\Phi}_- \left(\frac{p}{\Delta}\right) + \chi_{reg} \quad (53)$$

where $\tilde{\Phi}_- \left(\frac{p}{\Delta}\right)$ is a universal scaling function and χ_{reg} is the regular part. Since χ_{reg} is analytic across the transition, we can use the value of χ_{reg} obtained in the disordered phase, Eq. (36), as this allows us to identify the universal part unambiguously. This simplifies our analysis considerably.

Alternatively, one can repeat the analysis outlined in Sec. III to extract the universal part and the regular parts, without previous knowledge of χ_{reg} . Then, in order to extract the universal function unambiguously at $\mathcal{O}(\varepsilon^0)$ one must determine the logarithmic UV divergences to $\mathcal{O}(\varepsilon^1)$. This is a difficult calculation (see App. A). We have carried out this procedure, and found that indeed the value of χ_{reg} obtained in this manner matches the disordered phase, providing a very valuable consistency check of our calculations.

In order to obtain the universal scaling function, we use the known value of χ_{reg} to rewrite Eq. (52) in the form

$$\begin{aligned} \Omega_\varepsilon^{-1} \chi_s &= - \left[\frac{4}{\alpha_1} + \frac{2(N+8)p^2}{p^2+m^2} \right] \left[\frac{1}{\varepsilon} - \alpha_1 \left(1 + \ln \frac{\Lambda^2}{m^2}\right) \right] \\ &\quad + N \frac{\alpha_2}{\alpha_1^2} + \frac{(N-1)p^4}{(p^2+m^2)^2} \left(1 + \ln \frac{m^2}{p^2}\right) \\ &\quad - \frac{2(p^2-2m^2)^2 \tanh^{-1} x_m}{(p^2+m^2)^2 x_m} \\ &\quad - \frac{m^2 p^2 (N+8)}{(p^2+m^2)^2} \left(1 + \ln \frac{\Lambda^2}{m^2}\right) + \Omega_\varepsilon^{-1} \chi_{reg}, \end{aligned} \quad (54)$$

where α_1 is given in Eq. (31) and χ_{reg} is given by Eq. (36). In the following step, we use Eq. (49) to eliminate m in favor of Δ in Eq. (52),

$$\begin{aligned} \Omega_\varepsilon^{-1} \chi_s &= - \left[\frac{4}{\alpha_1} + \frac{2(N+8)p^2}{p^2+2\Delta^2} \right] \left[\frac{1}{\varepsilon} - \alpha_1 \left(1 + \ln \frac{\Lambda^2}{2\Delta^2}\right) \right] \\ &\quad + N \frac{\alpha_2}{\alpha_1^2} - 2\Delta^2 p^2 \frac{(N+2) \ln 2 - (N+8)}{(p^2+2\Delta^2)^2} \\ &\quad + \frac{(N-1)p^4}{(p^2+2\Delta^2)^2} \left(1 + \ln \frac{2\Delta^2}{p^2}\right) \\ &\quad - \frac{2(p^2-4\Delta^2)^2 \tanh^{-1} \tilde{x}}{(p^2+2\Delta^2)^2 \tilde{x}} + \Omega_\varepsilon^{-1} \chi_{reg}, \end{aligned} \quad (55)$$

where $\tilde{x} = \frac{p}{\sqrt{p^2+8\Delta^2}}$.

We obtain the overall constant \mathcal{A}_- ,

$$\mathcal{A}_- = \Omega_\varepsilon \Lambda^{-2\alpha} (N-1) \frac{\pi}{4}. \quad (56)$$

which will be shown to agree with Eq. (13). Then,

$$\begin{aligned}\tilde{\Phi}_-\left(\frac{p}{\Delta}\right) &= -\frac{2^\alpha}{\varepsilon} \frac{4\mathcal{C}}{N-1} \left(4 + \frac{(N-4)p^2}{p^2 + 2\Delta^2}\right) \\ &\quad + \frac{4}{\pi} \frac{p^4}{(p^2 + 2\Delta^2)^2} \left(1 + \ln \frac{2\Delta^2}{p^2}\right) \\ &\quad + \frac{1}{(N-1)\pi} \frac{8\Delta^2 p^2}{(p^2 + 2\Delta^2)^2} \left(-1 + \frac{N+2}{N+8} \ln 2\right) \\ &\quad - \frac{8}{(N-1)\pi} \frac{(p^2 - 4\Delta^2)^2 \tanh^{-1} \tilde{x}}{(p^2 + 2\Delta^2)^2 \tilde{x}}.\end{aligned}\quad (57)$$

where $\mathcal{C} = \frac{1}{\alpha_1 \pi} \left(\frac{1}{\varepsilon} - \alpha_1 - \frac{\alpha_2}{\alpha_1}\right)$, as before. The constant term $-\frac{2^\alpha}{\varepsilon} \frac{16\mathcal{C}}{N-1}$ in $\tilde{\Phi}_-\left(\frac{p}{\Delta}\right)$ does not contribute to the imaginary part of $\tilde{\Phi}_-(-i\frac{\omega}{\Delta} + 0^+)$ and will be omitted below.

As a check of our results, we consider the $p \gg \Delta$ limit, where Eq. (37) is expected to hold. Indeed, we find that

$$\begin{aligned}\tilde{\Phi}_-\left(\frac{p}{\Delta}\right) &\rightarrow \frac{4N}{N-1} \left(-2^\alpha \mathcal{C} + \frac{1}{\pi} \ln \frac{p^2}{2\Delta^2}\right) \\ &\quad + \mathcal{O}\left(\frac{\Delta}{p}\right) + \mathcal{O}(\varepsilon) \\ &= -\frac{4N\mathcal{C}}{N-1} \left(\frac{p}{\Delta}\right)^{2\alpha} + \mathcal{O}\left(\frac{\Delta}{p}\right) + \mathcal{O}(\varepsilon),\end{aligned}\quad (58)$$

as expected to $\mathcal{O}(\varepsilon)$. Conversely, we consider the low energy limit $\omega \ll \Delta$. In this limit, the universal scaling function is expected to follow an asymptotic power-law behavior, $\Phi\left(\frac{\omega}{\Delta}\right) \propto \left(\frac{\omega}{\Delta}\right)^{4-\varepsilon}$, due to the production of pairs of Goldstone modes¹⁶. Indeed, by writing $p = -i\omega + 0^+$ in Eq. (57) and taking the limit $\omega \ll \Delta$, we find that the imaginary part becomes

$$\Phi_-\left(\frac{\omega}{\Delta}\right) \rightarrow \left(\frac{\omega}{\Delta}\right)^{4-\varepsilon} + \mathcal{O}(\varepsilon^1)$$

as expected to this order in ε . This justifies our choice of \mathcal{A}_- in Eq. (56), in agreement with the definition in Eq. (13). These are non-trivial consistency checks of our results.

The spectral function extracted directly from Eq. (57) diverges as $\omega \rightarrow \sqrt{2}\Delta$ in a non-integrable manner. This can be avoided by noting that Eq. (57) has the form of a Dyson expansion to $\mathcal{O}(\varepsilon^2)$,

$$\frac{1}{p^2 + 2\Delta^2 - \Sigma} = \frac{1}{p^2 + 2\Delta^2} + \frac{\Sigma}{(p^2 + 2\Delta^2)^2} + \mathcal{O}(\varepsilon^2).$$

Within $\mathcal{O}(\varepsilon^0)$, we can re-write

$$\tilde{\Phi}_-\left(\frac{p}{\Delta}\right) = \frac{-2^{\alpha+2}\mathcal{C} \frac{N-4}{N-1} p^2}{p^2 + 2\Delta^2 - \Sigma_s(p)}, \quad (59)$$

where

$$\begin{aligned}\Sigma_s(p) &= -\varepsilon \frac{p^2}{2} \frac{N-1}{N+8} \left(1 + \ln \frac{2\Delta^2}{p^2}\right) \\ &\quad - \varepsilon \Delta^2 \left(\frac{N+2}{N+8} \ln 2 - 1\right) \\ &\quad + \varepsilon \frac{(p^2 - 4\Delta^2)^2 \tanh^{-1} x_\Delta}{p^2 (N+8) x_\Delta}.\end{aligned}\quad (60)$$

In this form, Eq. (59) has a well behaved spectral function. The universal scaling function, $\Phi_-\left(\frac{\omega}{\Delta}\right)$, is then extracted from $\tilde{\Phi}_-\left(\frac{p}{\Delta}\right)$ through the relation $\Phi_-\left(\frac{\omega}{\Delta}\right) = \Im \left\{ \tilde{\Phi}_-\left(-i\frac{\omega}{\Delta}\right) \right\}$.

$\Phi_-\left(\frac{\omega}{\Delta}\right)$ is depicted in Fig. 4 for $N = 2$ and 3. $\Phi_-\left(\frac{\omega}{\Delta}\right)$ has a distinct peak which can be identified with the Higgs excitation. The position of the peak depends on ε . For $\varepsilon = 0$, which is the noninteracting limit, the peak is a delta function at the mean field value of the Higgs mass, $m_H/\Delta = \sqrt{2}$. As ε increases, the peak broadens and its position is shifted towards larger frequencies. At $\varepsilon = 1$, the Higgs peak occurs at $m_H/\Delta = 1.67$ ($N = 2$) and $m_H/\Delta = 1.64$ ($N = 3$).

C. The Higgs pole

1. $D = 4 - \varepsilon$ for general N

At $\varepsilon = 0$, the scaling function (59) has a pole at $\omega = ip = \sqrt{2}\Delta$. At small ε , the pole is shifted to the lower half complex plane, and a branch cut starting at $p = 0$ appears. In order to obtain this result, we note that for small ε the pole is expected to lie near the real axis at $\omega_{\text{pole}} = \sqrt{2}\Delta + \mathcal{O}(\varepsilon)$. Substituting this expression into the denominator of Eq. (59) and expanding to linear order in ε yields

$$\begin{aligned}\frac{\omega_{\text{pole}}}{\sqrt{2}\Delta} &= 1 + \varepsilon \left(\frac{(N+2) \ln 2 + 3\sqrt{3}\pi}{4(N+8)} - \frac{1}{4} \right) \\ &\quad - i\varepsilon \frac{\pi}{4} \frac{N-1}{N+8} + \mathcal{O}(\varepsilon^2)\end{aligned}\quad (61)$$

which, at small ε , has a dominant real component. At $\varepsilon = 1$, we find $\omega_{\text{pole}}/\Delta = 1.74 - 0.11i$ for $N = 2$, whereas $\omega_{\text{pole}}/\Delta = 1.70 - 0.20i$ for $N = 3$. These values match the position and width of the resonances plotted in Fig. 4, up to the corrections of order ε^2 in Eq. (61). Note that these values are smaller than found in previous analyses. For example, two separate QMC analyses found $m_H/\Delta = 2.1(3)$ for $N = 2$ and $m_H/\Delta = 2.2(3)$ for $N = 3$ ^{24,25}; and 3.3(8) for $N = 2$ and 3.2(8) for $N = 3$ ²³; whereas an NPRG analyses obtained $m_H/\Delta \approx 2.5$ for $N = 2$ ²⁶. Qualitatively, the results agree on the sign of the shift in the Higgs mass relative to the mean field value $\sqrt{2}\Delta$, and on the fact that the Higgs mass is similar for $N = 2$ and

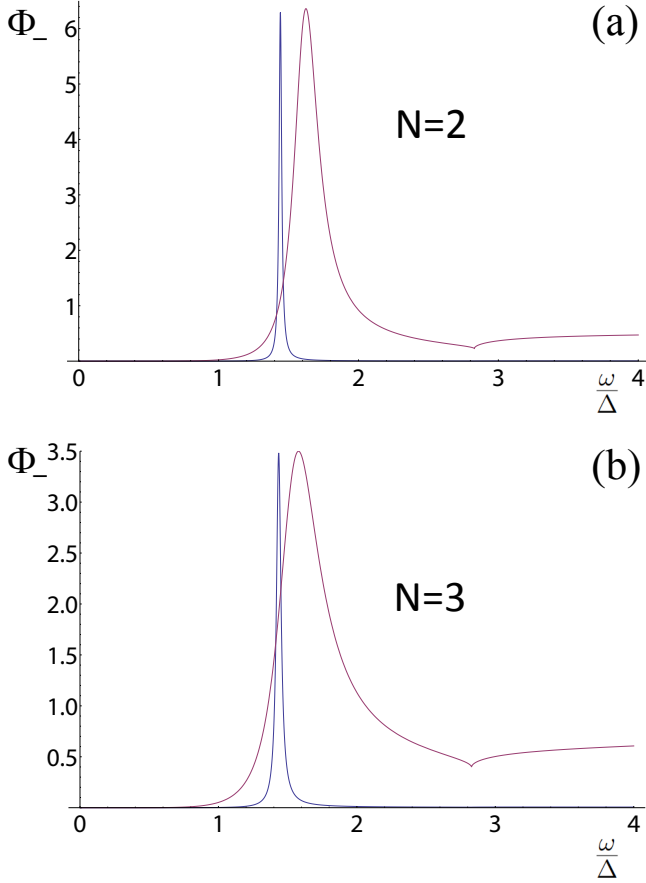


Figure 4: The universal scaling function in the ordered phase, $\Phi_-(-i\frac{\omega}{\Delta} + 0^+)$ to first order in ε , divided by $2^{\alpha+2}\mathcal{C}_{N-1}^{\frac{N-4}{N-1}}$. Results are for $\varepsilon = 0.1$ and $\varepsilon = 1$, for $N = 2$ (panel (a)) and $N = 3$ (panel (b)). Φ_- has a distinct peak which corresponds to the Higgs excitation. As ε is increased, the peak broadens and its position is shifted towards higher frequencies. At the threshold $\omega = 2\sqrt{2}\Delta$, there exists a small kink which is expected to be smoothed out at higher orders in ε .

$N = 3$. Quantitatively, the comparison of Higgs masses is not straightforward since higher order corrections to our results may be significant at $\varepsilon = 1$. We note that there is substantial disagreement between the different numerical analysis, and that our results are easier to reconcile with the lower of those results.

From the real and imaginary parts of Eq. (61) we can read off the Higgs mass m_H and its decay rate Γ_H , respectively. This yields the universal ratios:

$$\frac{m_H}{\sqrt{2}\Delta} = 1 + \varepsilon \left(\frac{(N+2)\ln 2 + 3\sqrt{3}\pi}{4(N+8)} - \frac{1}{4} \right), \quad (62)$$

$$\frac{\Gamma_H}{\sqrt{2}\Delta} = \varepsilon \frac{\pi}{4} \frac{N-1}{N+8}. \quad (63)$$

At this order in ε , m_H/Δ is monotonically decreasing with N for all $\varepsilon > 0$, whereas it increases with ε for

$N < 32$. On the other hand, Γ_H/Δ grows with ε , leading to a broadening of the resonance with lower dimension, as expected from the increased coupling strength as we move away from the Gaussian fixed point at $D = 3 + 1$. In addition, the width of the resonance grows with N , reflecting the larger number of Goldstone modes into which the Higgs mode can decay. The ratio m_H/Γ_H therefore grows monotonically with N , but is found to saturate at large N .

A previous NPRG calculation²⁶ found that in two spatial dimensions ($\varepsilon = 1$), the Higgs mode yields a distinct peak for $N = 2$, but that it is strongly suppressed for $N \geq 3$. By contrast, QMC simulations found a Higgs peak for both $N = 2$ and $N = 3$ ^{24,25}. In our analysis, we find that for $\varepsilon < \frac{4}{1+\pi-\ln 2} \approx 1.159$, the ratio m_H/Γ_H is larger than one for all values of N , indicating that the resonance exists for any value of N . However, for $\varepsilon > 1.159$, the condition $m_H/\Gamma_H > 1$ is no longer satisfied for large values of N , and therefore is possible that a calculation to higher orders in ε could change this picture.

A similar analytic structure was also found in a large N analysis in $D = 2 + 1$ dimensions²¹. There, it was obtained that at $N \rightarrow \infty$, $\omega_{\text{pole}} = -4i\Delta/\pi$ is purely imaginary at $D = 2 + 1$. In the large N expansion, the pole moves away from the imaginary axis, where the deviation from the imaginary axis is of $\mathcal{O}(\frac{1}{N})$. We will now study the evolution of ω_{pole} with the dimension of the system in the $N \rightarrow \infty$ limit.

2. $N \rightarrow \infty$ for general D

Following Ref.²¹ we can use a Hubbard-Stratonovich transformation to write the action in the ordered phase, Eq. (2), in the form,

$$\mathcal{Z} = \int \mathcal{D}\sigma \mathcal{D}\lambda \exp(-S_0), \quad (64)$$

where

$$S_0 = \int \frac{d^D p}{(2\pi)^D} [p^2 \sigma^2 + 2i\sigma_0 \sigma \lambda + \frac{1}{2} \left(\Pi_D(p, 0) + \frac{2}{NU} \right) \lambda^2 + \mathcal{O}\left(\frac{1}{N}\right)]. \quad (65)$$

Here, σ_0 is given by

$$\begin{aligned} \sigma_0^2 &= \int \frac{d^D p}{(2\pi)^D} \frac{1}{p^2} - \int \frac{d^D p}{(2\pi)^D} \frac{1}{p^2 + r} \\ &= -\frac{\pi}{2} \frac{K_D}{\sin(\frac{\pi D}{2})} r^{-1+D/2}. \end{aligned} \quad (66)$$

and

$$\Pi_D(p, 0) = (2-D) \frac{\pi}{4} \frac{p^{D-4} K_D \Gamma(\frac{D}{2}-1)^2}{\sin(\frac{\pi D}{2}) \Gamma(D-2)} \quad (67)$$

is the massless polarization bubble in a general space-time dimension D . Note that in this section, we use dimensional regularization in order to regularize UV divergencies.

The scalar susceptibility is related to the two point function of the λ field²¹ by the equation

$$\chi_s(p) = \frac{4N}{U} \left(1 - \frac{N}{U} G_{\lambda\lambda}(p) \right), \quad (68)$$

where the bare connected Green's function for the λ field is given by

$$G_{\lambda\lambda}(p) = \frac{2p^2}{\frac{p^2}{2} (\Pi_D(p, 0) + \frac{2}{NU}) + 2\sigma_0^2}. \quad (69)$$

As a consistency check with our $D = 4 - \varepsilon$ calculation, we find that for small ε and in the large N limit, Eqs. (59) and (69) agree up to an overall constant. Following the scheme which is outlined in Ref.²¹, we omit from Eq. (69) the term $\frac{2}{NU}$, which is negligible compared to $\Pi_D(p, 0)$ at small p .

Let us now explore the evolution of the $N \rightarrow \infty$ pole as we change the space-time dimension from $D = 2 + 1$ to $D = 3 + 1$. In the $N \rightarrow \infty$ limit, $r_c = 0$ and we can obtain the equation for the quasi-particle pole by applying the relations

$$\delta r = r = \Delta^2 + \mathcal{O}\left(\frac{1}{N}\right) \quad (70)$$

together with Eq. (66). We insert Eqs. (66), (67) and (70) into Eq. (69) to obtain that for a general space-time dimension D ,

$$\frac{\omega_{\text{pole}}}{2\Delta} = \left[\frac{i^D}{\pi^{3/2}} \Gamma\left(\frac{2-D}{2}\right) \Gamma\left(\frac{D-1}{2}\right) \sin \frac{\pi D}{2} \right]^{\frac{1}{D-2}}. \quad (71)$$

As expected, we find that at $D = 2 + 1$, $\omega_{\text{pole}} = -4i\Delta/\pi$ is purely imaginary. As D is increased from $D = 2 + 1$ to $D = 3 + 1$, ω_{pole} acquires a real part which becomes more dominant as D approaches 4, where $\omega_{\text{pole}} = \sqrt{2}\Delta$ becomes purely real, see Fig. 5. This demonstrates that the pole obtained in a $1/N$ expansion at $D = 2 + 1$ in Ref.²¹ can indeed be identified with the Higgs mode, as it smoothly evolves with dimension to the sharply-defined Higgs resonance at $D = 3 + 1$.

V. QUANTUM CRITICAL REGIME

We extend the calculation of the scalar susceptibility to the quantum critical regime, at temperature $T > 0$ and along the line $\delta r = 0$ (see Fig. 6). Since the order parameter vanishes in this regime, the formalism is similar to that given in Sec. III. The calculations at $T > 0$ are performed by discretizing the q^0 component of the Euclidean energy-momentum vector in Matsubara frequencies,

$$\mathbf{q} = (\omega_n, \vec{q}) \quad (72)$$

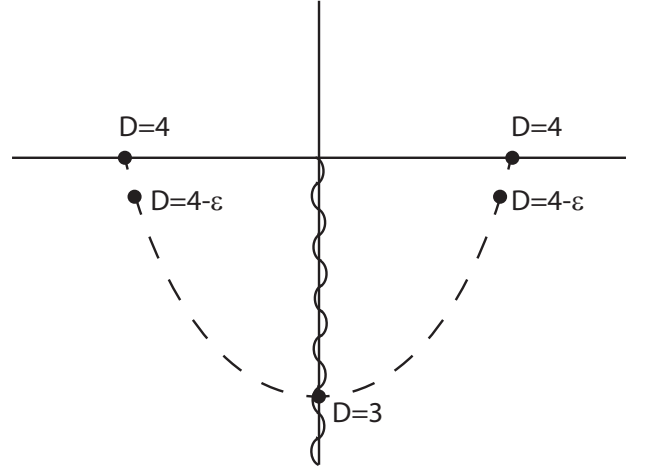


Figure 5: Analytic structure of the universal scaling function $\Phi_-(\omega)$ in the complex ω plane, in the $N \rightarrow \infty$ limit. In addition to a branch cut starting at $\omega = 0$, there are poles in the lower half plane whose positions depend on the space time dimension D . Note that the poles appear as partners on mirror positions on either side of the branch cut. For $D = 3 + 1$, the pole lies on the real axis, at $\sqrt{2}\Delta$. For $D = 2 + 1$ and $N = \infty$, $\omega_{\text{pole}} = -4i\Delta/\pi$ is purely imaginary. For $D = 2 + 1$ and large but finite N , the pole is shifted away from the imaginary axis²¹ by an amount of $\mathcal{O}(\frac{1}{N})$.

with $\omega_n = 2\pi nT$, where n is an integer. The integral dq_0 is then replaced by a sum,

$$\int \frac{d^{4-\varepsilon}q}{(2\pi)^{4-\varepsilon}} \rightarrow T \sum_{n=-\infty}^{\infty} \int \frac{d^{3-\varepsilon}q}{(2\pi)^{3-\varepsilon}}. \quad (73)$$

At $T > 0$, thermal fluctuations shift the location of the critical point to enlarge the disordered phase, see Fig. 6. The resulting correction to the self energy of the ϕ field is, to first order,

$$\begin{aligned} \Sigma &= -\frac{U_c(N+2)}{2} \left[T \sum_{\omega_n} \int \frac{d^{3-\varepsilon}q}{(2\pi)^{3-\varepsilon}} \frac{1}{\omega_n^2 + \vec{q}^2} \right. \\ &\quad \left. - \int \frac{d^{4-\varepsilon}q}{(2\pi)^{4-\varepsilon}} \frac{1}{q^2} \right] \\ &= -\varepsilon \frac{N+2}{N+8} \frac{T^2}{12K_4} + \mathcal{O}(\varepsilon^2) \equiv -m_T^2. \end{aligned} \quad (74)$$

The transition then occurs when $\delta r - \Sigma = 0$, which corresponds to $\delta r = -m_T^2$. Conversely, at $\delta r = 0$ the ϕ propagator has an effective mass m_T ,

$$G(\omega_n, \vec{q}; \delta r = 0, T) = \frac{1}{\omega_n^2 + \vec{q}^2 + m_T^2} + \mathcal{O}(\varepsilon^2). \quad (75)$$

Note that if higher order corrections are included, the self energy is expected to become momentum dependent.

We next turn to evaluate the scalar susceptibility. The formal expression for χ_{scalar} in the disordered phase was

obtained in terms of the polarization bubble $\Pi(p, \delta r)$ in Sec. III C. This result can be generalized to finite temperatures by replacing $\Pi(p, \delta r)$ with $\Pi_T(\omega_n, \vec{p}, \delta r)$ in Eq. (26),

$$\chi_s(\omega_n, \vec{p}, T) = 2N\Pi_T(\omega_n, \vec{p}, \delta r) - U_c N(N+2)\Pi_T(\omega_n, \vec{p}, \delta r)^2 + \mathcal{O}(\varepsilon^2). \quad (76)$$

Here, $\Pi_T(\omega_n, \vec{p}, \delta r)$ is the polarization bubble at finite temperatures. We focus on $\vec{p} = 0$ and $\delta r = 0$. The formal expression for $\Pi_T^0(\omega_n) \equiv \Pi_T(\omega_n, \vec{p} = 0, \delta r = 0)$ is then

$$\Pi_T^0(\omega_n) = \frac{T}{(2\pi)^3} \sum_m \int \frac{d^{3-\varepsilon}q}{(2\pi)^3} \frac{1}{\omega_m^2 + \vec{q}^2 + m_T^2} \times \frac{1}{(\omega_m - \omega_n)^2 + \vec{q}^2 + m_T^2}, \quad (77)$$

Temperature has the effect of regularizing IR divergences. However, it has no effect on UV divergences, which must therefore be the same for $\Pi_T^0(\omega_n, \vec{p})$ and $\Pi(p, \Delta)$, Eq. (27). This implies that $\Pi_T^0(\omega_n)$ can be written in the form

$$\Omega_\varepsilon^{-1} \Pi_T^0(\omega_n) = \pi_0(\omega_n) \left(1 + \frac{\varepsilon}{2} \left(1 + \ln \frac{\Lambda^2}{T^2} \right) \right) + \frac{1}{2} \ln \frac{\Lambda^2}{T^2} + \frac{\varepsilon}{8} \ln^2 \frac{\Lambda^2}{T^2} + \varepsilon \pi_1(\omega_n) + \mathcal{O}(\varepsilon^2) \quad (78)$$

where π_0 and π_1 are functions that are independent of the cutoff and of ε , as we have verified explicitly.

We can now obtain the general form of the scalar susceptibility for $T > 0$ by inserting Eq. (78) into Eq. (26),

$$\begin{aligned} \frac{\Omega_\varepsilon^{-1}}{N} \chi_s(\omega_n, T) &= \ln \frac{\Lambda^2}{T^2} - \frac{1}{2} \alpha_1 \varepsilon \ln^2 \frac{\Lambda^2}{T^2} \\ &+ 2\pi_0 \left(1 - \alpha_1 \varepsilon \ln \frac{\Lambda^2}{T^2} \right) \\ &- \varepsilon (1 + 2\alpha_1) \pi_0^2 \\ &+ \varepsilon (2\pi_1 + \pi_0) + \mathcal{O}(\varepsilon^2). \end{aligned} \quad (79)$$

We extract the universal scaling function from Eq. (79) by proceeding in line with Sec. III D. As before, we obtain a logarithmic dependence on Λ with prefactor of order ε^0 . This motivates us to choose $\mathcal{A}_T = \mathcal{A}_+$, as given in Eq. (33). We find that

$$\begin{aligned} \Phi_T \left(\frac{\omega}{T} \right) &= \frac{2}{\pi} \left(\pi_0''(\omega) + \varepsilon \pi_1''(\omega) \right) \\ &- \frac{2}{\pi} \varepsilon (1 + 2\alpha_1) \pi_0'(\omega) \pi_0''(\omega) \\ &+ \varepsilon \alpha_1 + \frac{\varepsilon}{2} \ln 2 + \mathcal{O}(\varepsilon^2). \end{aligned} \quad (80)$$

where $\pi_0' = \Re\{\pi_0(-i\omega + 0^+)\}$, $\pi_0'' = \Im\{\pi_0(-i\omega + 0^+)\}$ and $\pi_1'' = \Im\{\pi_1(-i\omega + 0^+)\}$. In order to obtain the

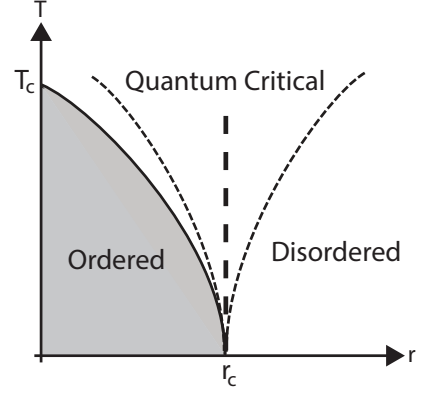


Figure 6: The phase diagram of the $O(N)$ model in the $r - T$ plane. We present results along the thick dashed line.

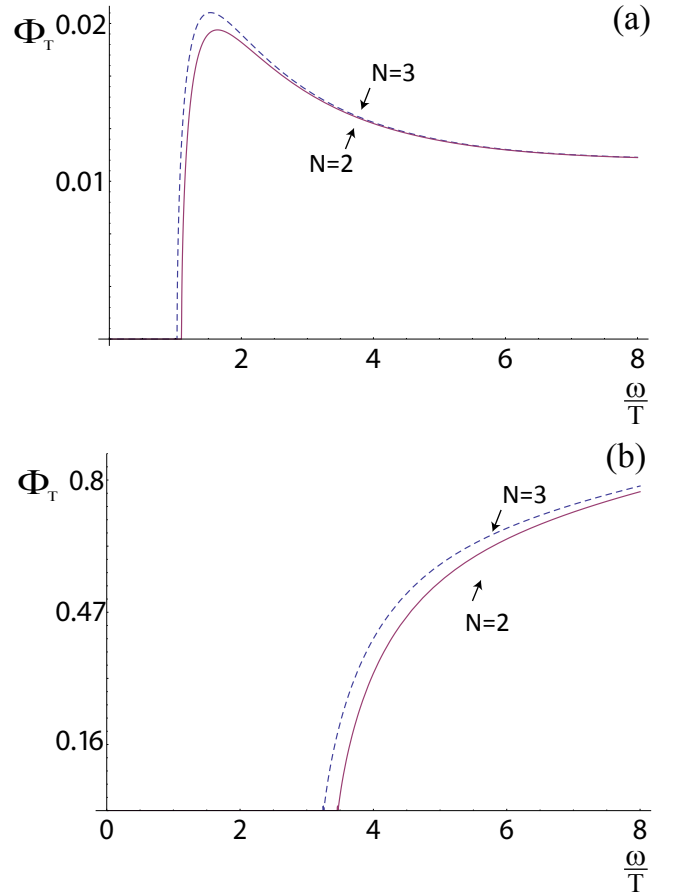


Figure 7: The universal scaling function in the quantum critical regime, $\Phi_T \left(\frac{\omega}{T} \right)$, to second order in ε , divided by N . Results are for $\varepsilon = 0.1$ (panel (a)), $\varepsilon = 1$ (panel (b)) and for $N = 2, 3$.

explicit form of Eq. (80), we are left to calculate π_0' , π_0'' and π_1'' . The calculation of the latter two is given in Appendix B, while π_0' is obtained numerically. We find

$$\pi_0''(\omega) = \Theta(|\omega| - 2m_T) \frac{\pi \sqrt{\omega^2 - 4m_T^2}}{2|\omega|} \coth \frac{\omega}{4T}, \quad (81)$$

$$\pi_1''(\omega) = -\pi_0''(\omega) \times \frac{1}{2} \ln \left| \frac{\omega^2}{4} - m_T^2 \right|. \quad (82)$$

We can now obtain the explicit form of the universal scaling function for $T > 0$, to second order in ε , by inserting Eqs. (81) and (82) into Eq. (80),

$$\begin{aligned} \Phi_T \left(\frac{\omega}{T} \right) &= \Theta(|\omega| - 2m_T) \frac{\sqrt{\omega^2 - 4m_T^2}}{|\omega|} \coth \frac{\omega}{4T} \\ &\times \left[1 - 2\varepsilon (1 + 2\alpha_1) \pi_0'(\omega) \right. \\ &\left. + \frac{\varepsilon}{2} \ln \left| \frac{\omega^2}{4} - m_T^2 \right| \right] + \mathcal{O}(\varepsilon^2). \end{aligned} \quad (83)$$

As a consistency check, we find that in the high frequency limit, $\omega \gg T$, Eq. (83) yields the expected scaling form, $\Phi_T \propto (\omega/T)^{2\alpha}$.

Equation (83) is plotted in Fig. 7. For $\varepsilon = 0.1$, the response function $\Phi_T(\frac{\omega}{T})$ exhibits a Higgs-like peak near the threshold. However, this peak broadens as ε is increased and is no longer present at $\varepsilon = 1$.

Note that $\Phi_T(\frac{\omega}{T})$ has a threshold at $\omega = 2m_T$. Unlike the threshold at $T = 0$ in the disordered phase, which is a consequence of the gap in the spectrum in that case, in the quantum critical regime the spectrum is gapless and hence no such threshold is expected. In fact, the threshold is an artifact of our working order, in which the mass term m_T is independent of momentum, hence playing the role of a hard gap. At two loop level, the self energy becomes momentum dependent, hence smearing the threshold. This calculation is difficult and it may not be possible to extract the low frequency response function for $\omega < \sqrt{\varepsilon}T$ reliably from such a calculation³³. However, QMC simulations for $N = 3$ indicate that the quasiparticle width in the quantum critical region is small, and hence a threshold-like effect may still exist even after higher order corrections are taken into account³⁴.

VI. SUMMARY AND DISCUSSION

We have studied the Higgs mode of the relativistic $O(N)$ model near $D = 3 + 1$ spacetime dimensions by computing the scalar spectral function through a controlled expansion in the small parameter $\varepsilon = 4 - D$, and extracting the universal scaling function near the quantum phase transition between the ordered and disordered phases.

In the ordered phase, the spectral function has a complex pole associated with a sharp Higgs resonance. The

pole occurs at a strictly real frequency at $D = 3 + 1$, and acquires a small imaginary component for $D = 4 - \varepsilon$. Previous work computed the scalar susceptibility in the large N limit and found a pole corresponding to a damped excitation at $D = 2 + 1$, which was identified with the Higgs resonance²¹. Indeed, we show that for $N \rightarrow \infty$, this pole evolves smoothly with D to the sharp Higgs mode seen at $D = 4 - \varepsilon$.

Our analysis predicts a sharp Higgs mode in three spatial dimensions close to the critical point. However, this does not indicate that the Higgs mode has zero width in realistic experiments^{8,35}. While our calculation applies asymptotically close to the QCP, for $D = 3 + 1$ the relative width of the Higgs mode approaches zero only logarithmically in δr , and hence even relatively close to the QCP, the Higgs resonance has a finite width^{19,35}.

In the disordered phase, we have found that the scalar spectral function has a threshold at $\omega = 2\Delta$ and no Higgs-like peak. This outcome is in disagreement with a previous QMC analysis which found a peak close to the threshold, which was interpreted as a precursor to the Higgs mode in the disordered phase²³. A weak peak in the spectral function was also found in a separate QMC analysis²⁵, as well as in a NPRG calculation²⁶. However, the spectral weight of this peak is much smaller than that of the Higgs peak on the ordered side. We note, furthermore, that these analyses rely on numerical analytic continuation, which is difficult to control and which is liable to yield spurious oscillations when the spectral function changes rapidly³⁶. Of course, our calculation is only controlled for small ε , and it cannot conclusively rule out such a peak for $D = 2 + 1$. Finally, we note that even if such a peak were to be present, renormalization group arguments show that it should not be interpreted as a precursor to the Higgs mode²⁶. Instead, such a peak could be an indication of an emergent bound state of gapped particle-hole excitations in the disordered phase near the QCP.

Finally, we computed the universal spectral function in the quantum critical regime. For $\varepsilon \ll 1$, we find indirect evidence for a peak in the spectral function at ω of order T , which may agree with Ref.²³, although for $\varepsilon = 1$ no such peak is seen. Instead, only a threshold-like behavior is observed at low frequencies.

It would be interesting to apply these methods to study other dynamical properties such as the reactive conductivity³⁷ near quantum criticality in $D = 4 - \varepsilon$ dimensions.

Acknowledgments

We would like to thank Shmuel Fishman, Snir Gazit, Adam Rancon, Subir Sachdev, and William Witczak-Krempa for useful discussions. D. P. acknowledges support from an Israeli Science Foundation grant and from a joint grant of the Israel Science Foundation and the Indian University Grant Commission. We thank the As-

pen Center for Physics, where part of this work was completed.

Appendix A: Scalar Susceptibility in the Ordered Phase

We calculate the scalar susceptibility in the ordered phase to $\mathcal{O}(\varepsilon)$ by computing the different correlation functions in Eq. (51). This requires calculation of $\chi_{\pi^2\pi^2}$, $\chi_{\sigma^2\sigma^2}$ and $\chi_{\pi^2\sigma^2}$ to $\mathcal{O}(\varepsilon)$, $\chi_{\pi^2\sigma}$ and $\chi_{\sigma^2\sigma}$ to $\mathcal{O}(\varepsilon^{3/2})$, and $\chi_{\sigma\sigma}$ to $\mathcal{O}(\varepsilon^2)$. The full diagrammatic expansion of this procedure is presented in Fig. 9, where our notations for the Feynman diagrams is shown in Fig. 8. We find

$$\chi_{\pi^2\pi^2} = (N-1) \left\{ 2\Pi(p,0) + U_c(N-1) \left[2E(p,0) + 4L(p) + \left(\frac{(N-1)m^2}{p^2+m^2} - N-1 \right) \Pi(p,0)^2 \right] \right\}, \quad (\text{A1})$$

$$\chi_{\sigma^2\sigma^2} = 2\Pi(p,m) + 2U_c \left[-\frac{3p^2-2m^2}{2(p^2+m^2)} \Pi(p,m)^2 + 9(E(p,m) + F(p,m)) + (N-1)F(p,0) \right], \quad (\text{A2})$$

$$\chi_{\pi^2\sigma^2} = 2U_c(N-1) \left[-\frac{p^2-2m^2}{p^2+m^2} \Pi(p,m) \Pi(p,0) + 2G(p) \right], \quad (\text{A3})$$

$$\begin{aligned} 4\frac{m}{\sqrt{U_c}}\chi_{\sigma^2\sigma} = & -\frac{12m^2}{p^2+m^2}\Pi(p,m) + U_c\frac{4m^2}{p^2+m^2} [27(E(p,m) + F(p,m)) - (N-1)(E(p,0) + 3F(p,0))] \\ & + 2U_c\frac{m^2(p^2-2m^2)}{(p^2+m^2)^2} [(N-1)\Pi(p,0) + 9\Pi(p,m)] \Pi(p,m), \end{aligned} \quad (\text{A4})$$

$$\begin{aligned} 4\frac{m}{\sqrt{U_c}}\chi_{\pi^2\sigma} = & 2(N-1)m^2 \left[\left(\frac{-2}{p^2+m^2} + U_c\frac{(N+1)p^2+2m^2}{(p^2+m^2)^2} \Pi(p,0) + 3U_c\frac{p^2-2m^2}{(p^2+m^2)^2} \Pi(p,m) \right) \Pi(p,0) \right. \\ & \left. - U_c\frac{2(N-1)}{p^2+m^2} (E(p,0) + 2L(p) + 3G(p)) \right], \end{aligned} \quad (\text{A5})$$

$$\begin{aligned} 4\frac{m^2}{U_c}\chi_{\sigma\sigma} = & \frac{4}{U_c}\frac{m^2}{p^2+m^2} + \frac{m^4}{(p^2+m^2)^2} \{ 2(N-1)\Pi(p,0) + 18\Pi(p,m) + U_c[162(E(p,m) + F(p,m)) \\ & 3\frac{p^2-2m^2}{p^2+m^2} (9\Pi(p,m)^2 + (N-1)\Pi(p,m)\Pi(p,0)) - \frac{(N^2-1)p^2+2(N-1)m^2}{(p^2+m^2)} \Pi(p,0)^2 \\ & + 6K(p,m) + 2(N-1)(E(p,0) + 6G(p) + 2L(p) + 9F(p,0) + K(p,0))] \}, \end{aligned} \quad (\text{A6})$$

where

$$\Pi(p,0) = K_{4-\varepsilon} \left[\frac{1}{2} \left(1 + \ln \frac{\Lambda^2}{p^2} \right) + \frac{1}{8} \varepsilon \left(1 + \ln \frac{\Lambda^2}{p^2} \right)^2 + \frac{3}{8} \varepsilon \right] + \mathcal{O}(\varepsilon^2), \quad (\text{A7})$$

and

$$\begin{aligned} E(p, m_0) &= m^2 \int_{k,q} \frac{1}{q^2+m_0^2} \frac{1}{(\mathbf{q}+\mathbf{p})^2+m_0^2} \frac{1}{k^2+m_0^2} \frac{1}{(\mathbf{k}+\mathbf{p})^2+m_0^2} \frac{1}{(\mathbf{k}+\mathbf{q})^2+m^2}, \\ G(p) &= m^2 \int_{k,q} \frac{1}{q^2} \frac{1}{(\mathbf{q}+\mathbf{p})^2} \frac{1}{(\mathbf{k}+\mathbf{p})^2+m^2} \frac{1}{(\mathbf{k}-\mathbf{q})^2} \frac{1}{k^2+m^2}, \\ L(p) &= m^2 \int_{k,q} \frac{1}{q^4} \frac{1}{(\mathbf{q}+\mathbf{p})^2} \frac{1}{(\mathbf{k}+\mathbf{q})^2} \frac{1}{k^2+m^2}, \\ F(p, m_0) &= m^2 \int_k \frac{\Pi(k, m_0)}{(k^2+m^2)^2} \frac{1}{(\mathbf{k}+\mathbf{p})^2+m^2}, \\ K(p, m_0) &= \frac{1}{m^2} \int_k \frac{\Pi(k, m_0)}{(\mathbf{k}+\mathbf{p})^2+m^2}. \end{aligned} \quad (\text{A8})$$

The integrals $E(p, m)$ and $G(p)$ are independent of the UV cutoff. The remaining terms can be written as

$$\begin{aligned}
L(p) &= K_{4-\varepsilon}^2 \left[\frac{m^2}{4p^2} \left(1 + \ln \frac{\Lambda^2}{m^2} \right) + \frac{m^2}{4p^2} \ln \frac{p^2}{p_0^2} \ln \frac{\Lambda^2}{m^2} + \Delta L \right], \\
F(p, m) &= K_{4-\varepsilon}^2 \left[\frac{m^2}{p^2+m^2} \frac{\tanh^{-1} x_m}{2x_m} \left(1 + \ln \frac{\Lambda^2}{m^2} \right) + \Delta F_1 \right], \\
F(p, 0) &= K_{4-\varepsilon}^2 \left[\frac{m^2}{p^2+m^2} \frac{\tanh^{-1} x_m}{2x_m} \left(1 + \ln \frac{\Lambda^2}{m^2} \right) + \Delta F_2 \right], \\
K(p, m) &= K_{4-\varepsilon}^2 \left[\frac{2\Lambda^2}{m^2} + \frac{p^2-m^2}{2m^2} \left(1 + \ln \frac{\Lambda^2}{m^2} \right)^2 + \frac{m^2-2p^2}{m^2} \left(1 + \ln \frac{\Lambda^2}{m^2} \right) + \Delta K_1 \right] \\
K(p, 0) &= K_{4-\varepsilon}^2 \left[\frac{2\Lambda^2}{m^2} + \frac{p^2-m^2}{2m^2} \left(1 + \ln \frac{\Lambda^2}{m^2} \right)^2 + \frac{m^2-2p^2}{m^2} \left(1 + \ln \frac{\Lambda^2}{m^2} \right) + \Delta K_2 \right]
\end{aligned} \tag{A9}$$

where p_0 is an IR cutoff on momentum, introduced to regulate $L(p)$. The terms $\Delta L, \Delta F_1, \Delta F_2, \Delta K_1$ and ΔK_2 are independent of the UV cutoff and are given by

$$\Delta L = \frac{m^2}{4p^2} \text{Li}_2 \left(-\frac{p^2}{m^2} \right) - \frac{3m^2}{8p^2} + \frac{1}{8} \ln \frac{p^2}{m^2+p^2} - \frac{m^4}{8p^4} \ln \frac{m^2}{m^2+p^2} \tag{A10}$$

$$\Delta F_1 = \frac{1}{K_{4-\varepsilon}} \int_q \frac{\frac{\sqrt{q^2+4m^2}}{q} \tanh^{-1} \frac{q}{\sqrt{q^2+4m^2}}}{((\mathbf{p}+\mathbf{q})^2+m^2)(q^2+m^2)^2}, \tag{A11}$$

$$\Delta F_2 = \frac{1}{K_{4-\varepsilon}} \int_q \frac{\frac{\sqrt{q^2+4m^2}}{q} \ln \frac{m^2}{q^2}}{((\mathbf{p}+\mathbf{q})^2+m^2)(q^2+m^2)^2}, \tag{A12}$$

$$\Delta K_1 = -\frac{2}{K_{4-\varepsilon}} \int_q \frac{\left(\frac{\sqrt{q^2+4m^2}}{q} \tanh^{-1} \frac{q}{\sqrt{4m^2+q^2}} - \frac{1}{2} \ln \frac{m^2}{q^2} \right)}{(\mathbf{p}+\mathbf{q})^2+m^2}, \tag{A13}$$

$$\Delta K_2 = \frac{m^2-p^2}{2m^2} \left(1 - 2\text{Li}_2 \left(\frac{m^2}{p^2} \right) - \ln^2 \frac{p^2}{m^2} + \frac{\pi^2}{6} \right) + \frac{2p^2}{m^2} \ln \frac{2p^2}{m^2} + 2 \ln 2 - 2. \tag{A14}$$

Note that the term $L(p)$ is IR divergent. This can be avoided by including the next order corrections to the counterterm of π^2 . However, this is not necessary here since we only extract the universal scaling function to order ε^0 , and therefore we are only interested in the UV divergences of the $L(p)$ term.

Summation of Eqs. (A1)-(A6) yields a formal expression for the scalar susceptibility to $\mathcal{O}(\varepsilon)$,

$$\begin{aligned}
\chi_s(p) &= \frac{4}{U_c} \frac{m^2}{p^2+m^2} + 2 \frac{(p^2-2m^2)^2}{(p^2+m^2)^2} \left\{ \Pi(p, m) - \frac{3}{2} U_c \frac{p^2-2m^2}{p^2+m^2} \Pi(p, m)^2 - U_c \frac{(N-1)p^2}{p^2+m^2} \Pi(p, m) \Pi(p, 0) \right. \\
&\quad \left. + U_c (9(E(p, m) + F(p, m)) + (N-1)F(p, 0)) \right\} + U_c \frac{2m^6}{(p^2+m^2)^3} (3K(p, m) + (N-1)K(p, 0)) \\
&\quad \left. + \frac{2(N-1)p^4}{(p^2+m^2)^2} \left\{ \Pi(p, 0) - U_c \left[\frac{2m^2+(N+1)p^2}{2(p^2+m^2)} \Pi(p, 0)^2 + 2L(p) + E(p, 0) + 2 \left(1 - 2 \frac{m^2}{p^2} \right) G(p) \right] \right\} \right\}.
\end{aligned} \tag{A15}$$

We can use this expression to obtain the logarithmic UV divergences at $\mathcal{O}(\varepsilon)$. From this, using Eq. (34), we extract the universal scaling function. Indeed, we find that the result of this analysis yields Eq. (57), and that the regular part χ_{reg} matches that obtained in the disordered phase, Eq. (36).

Appendix B: Polarization bubble at finite temperatures

We compute π_0'' and π_1'' , the imaginary parts of π_0 and π_1 , see Eq. (79). These terms are used in Sec. V in order to obtain the universal scaling function in the quantum critical regime.

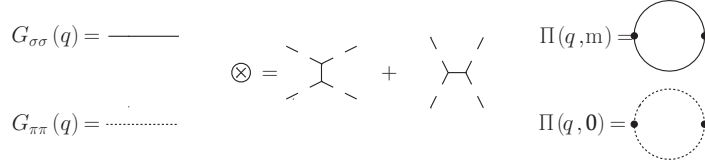


Figure 8: Notations for the Feynman Diagrams in the ordered phase. The cross represents the different ways to contract lines at the interaction vertex.

The sum in Eq. (77) can be performed by using the identity¹⁶

$$T \sum_m \frac{1}{\omega_m^2 + a^2} \frac{1}{(\omega_m + \omega_n)^2 + b^2} = \frac{n(-a)}{2a \left((i\omega_n - a)^2 - b^2 \right)} - \frac{n(a)}{2a \left((i\omega_n + a)^2 - b^2 \right)} + \frac{n(-b)}{2a \left((i\omega_n + b)^2 - a^2 \right)} - \frac{n(b)}{2a \left((i\omega_n - b)^2 - a^2 \right)} \quad (\text{B1})$$

where $n(\nu)$ is the Bose-Einstein occupation function,

$$n(\nu) = \frac{1}{\exp(\nu/T) - 1}. \quad (\text{B2})$$

We insert Eq. (B1) into Eq. (77) to obtain

$$\Pi_T^0(\omega_n) = K_{4-\varepsilon} \int_q \frac{1}{\sqrt{q^2 + m_T^2}} \frac{\coth \frac{\sqrt{q^2 + m_T^2}}{2T}}{q^2 + m_T^2 + \frac{\omega_n^2}{4}} q^2 d^d q \quad (\text{B3})$$

We are only interested in the finite part of Eq. (B3) to $\mathcal{O}(\varepsilon^0)$. We will therefore subtract the divergent part by writing

$$\pi_0(\omega_n) = \int_0^\infty \frac{1}{\sqrt{q^2 + m_T^2}} \left[\frac{\coth \frac{\sqrt{q^2 + m_T^2}}{2T}}{q^2 + \frac{\omega_n^2}{4} + m_T^2} - \frac{1}{q^2 + m_T^2} \right] q^2 dq. \quad (\text{B4})$$

We have normalized Eq. (B4) by $K_{4-\varepsilon}$ in order for $\pi_0(\omega_n)$ to be consistent with Eq. (78).

We now replace ω_n with real frequencies by performing a Wick rotation, $\omega_n \rightarrow -i\omega + 0^+$,

$$\pi_0(\omega) = \int_0^\infty \frac{1}{\sqrt{q^2 + m_T^2}} \left[\frac{\coth \frac{\sqrt{q^2 + m_T^2}}{2T}}{q^2 - \frac{\omega^2}{4} - i0^+ + m_T^2} \text{sign}(\omega) - \frac{1}{q^2 + m_T^2} \right] q^2 dq. \quad (\text{B5})$$

The imaginary part of Eq. (B5) can be computed by using the identity,

$$\frac{1}{x + i0^+} = \mathcal{P} \left(\frac{1}{x} \right) - i\pi \delta(x) \quad (\text{B6})$$

where \mathcal{P} denotes the principal value. We insert Eq. (B6) into Eq. (B5) to find

$$\pi_0''(\omega) = \pi \int_0^\infty \frac{1}{\sqrt{q^2 + m_T^2}} \coth \frac{\sqrt{q^2 + m_T^2}}{2T} \text{sign}(\omega) \delta \left(q^2 - \frac{\omega^2}{4} + m_T^2 \right) q^2 dq. \quad (\text{B7})$$

By performing the integral in Eq. (B7), we obtain

$$\pi_0''(\omega) = \frac{\pi}{2|\omega|} \sqrt{\omega^2 - 4m_T^2} \Theta(|\omega| - 2m_T) \coth \frac{\omega}{4T}. \quad (\text{B8})$$

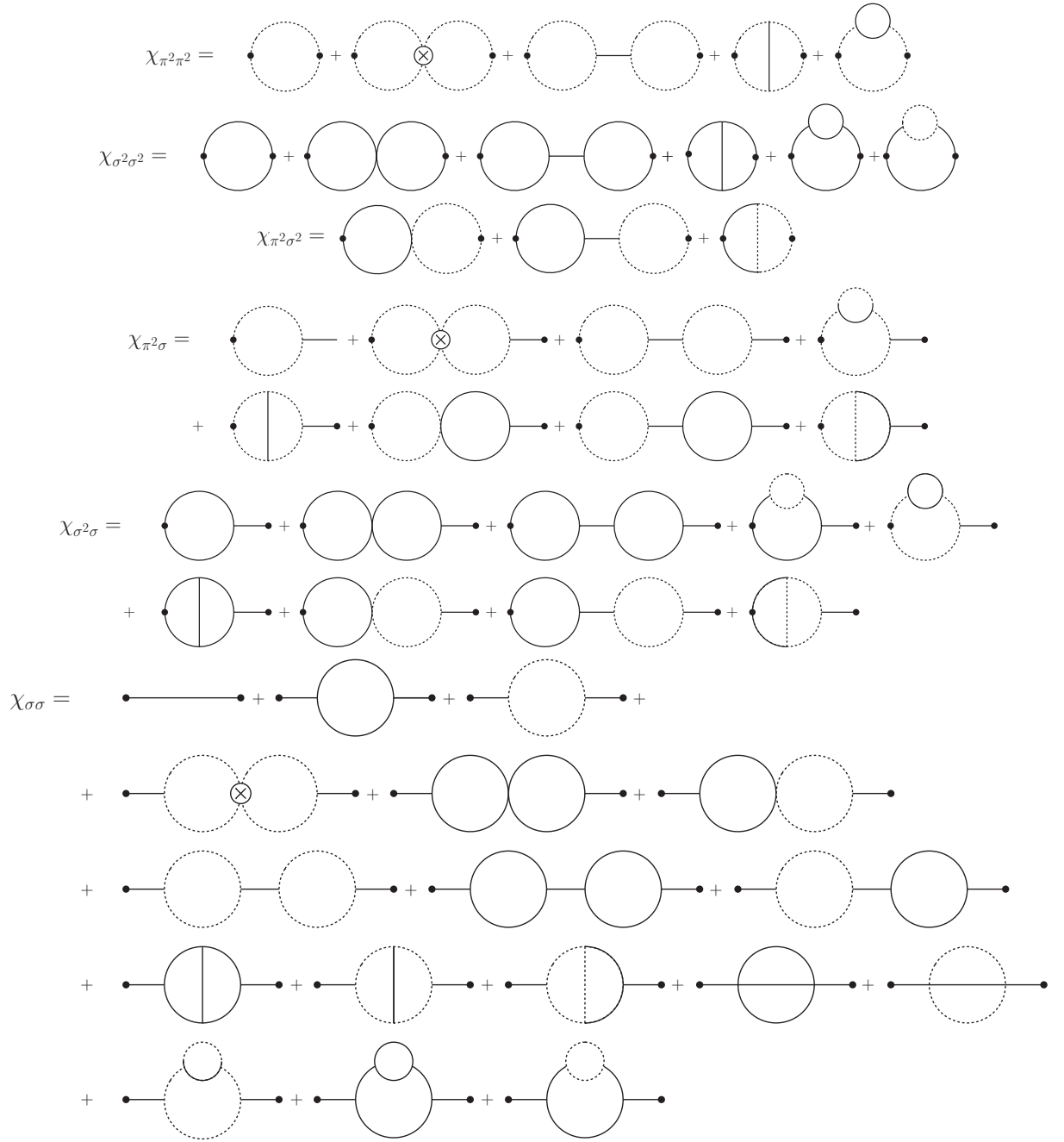


Figure 9: Diagrammatic expansion in ε , of the susceptibilities which compose the scalar susceptibility in the ordered phase. $\chi_{\pi^2\pi^2}, \chi_{\sigma^2\sigma^2}$ and $\chi_{\pi^2\sigma^2}$ are calculated to $\mathcal{O}(\varepsilon)$, $\chi_{\sigma^2\sigma}$ and $\chi_{\pi^2\sigma}$ to $\mathcal{O}(\varepsilon^{3/2})$ and $\chi_{\sigma\sigma}$ to $\mathcal{O}(\varepsilon^2)$.

We can obtain, in a similar manner,

$$\pi_1'' = -\frac{1}{2}\pi_0''(\omega) \ln \left| \frac{\omega^2}{4} - m_T^2 \right|. \quad (\text{B9})$$

¹ R. Coldea, D. A. Tennant, E. M. Wheeler, E. Wawrzynska, D. Prabhakaran, M. Telling, K. Habicht, P. Smeibidl, and

K. Kiefer, Science **327**, 177 (2010), ISSN 0036-8075, 1095-9203, PMID: 20056884, URL <http://www.sciencemag>.

- org/content/327/5962/177.
- ² S. Sachdev, K. Sengupta, and S. M. Girvin, *Physical Review B* **66**, 075128 (2002), URL <http://link.aps.org/doi/10.1103/PhysRevB.66.075128>.
 - ³ J. Simon, W. S. Bakr, R. Ma, M. E. Tai, P. M. Preiss, and M. Greiner, *Nature* **472**, 307 (2011), ISSN 0028-0836, URL <http://www.nature.com/nature/journal/v472/n7343/full/nature09994.html>.
 - ⁴ B. Grenier, S. Petit, V. Simonet, E. Canévet, L.-P. Regnault, S. Raymond, B. Canals, C. Berthier, and P. Lejay, *Phys. Rev. Lett.* **114**, 017201 (2015), URL <http://link.aps.org/doi/10.1103/PhysRevLett.114.017201>.
 - ⁵ I. B. Spielman, W. D. Phillips, and J. V. Porto, *Physical Review Letters* **98**, 080404 (2007), URL <http://link.aps.org/doi/10.1103/PhysRevLett.98.080404>.
 - ⁶ M. Endres, T. Fukuhara, D. Pekker, M. Cheneau, P. Schauß, C. Gross, E. Demler, S. Kuhr, and I. Bloch, *Nature* **487**, 454 (2012), ISSN 0028-0836, URL <http://www.nature.com/nature/journal/v487/n7408/full/nature11255.html>.
 - ⁷ D. S. Chow, P. Wzietek, D. Fogliatti, B. Alavi, D. J. Tantillo, C. A. Merlic, and S. E. Brown, *Physical Review Letters* **81**, 3984 (1998), URL <http://link.aps.org/doi/10.1103/PhysRevLett.81.3984>.
 - ⁸ C. Rüegg, B. Normand, M. Matsumoto, A. Furrer, D. F. McMorrow, K. W. Krämer, H. U. Güdel, S. N. Gvasaliya, H. Mutka, and M. Boehm, *Physical Review Letters* **100**, 205701 (2008), URL <http://link.aps.org/doi/10.1103/PhysRevLett.100.205701>.
 - ⁹ C. Varma, *Journal of Low Temperature Physics* **126**, 901 (2002), ISSN 0022-2291, URL <http://dx.doi.org/10.1023/A%3A1013890507658>.
 - ¹⁰ D. Pekker and C. Varma, arXiv preprint arXiv:1406.2968 (2014).
 - ¹¹ S. Sachdev, *Physical Review B* **59**, 14054 (1999), URL <http://link.aps.org/doi/10.1103/PhysRevB.59.14054>.
 - ¹² W. Zwerger, *Physical Review Letters* **92**, 027203 (2004), URL <http://link.aps.org/doi/10.1103/PhysRevLett.92.027203>.
 - ¹³ N. Dupuis, *Physical Review E* **83**, 031120 (2011), URL <http://link.aps.org/doi/10.1103/PhysRevE.83.031120>.
 - ¹⁴ A. V. Chubukov, S. Sachdev, and J. Ye, *Physical Review B* **49**, 11919 (1994), URL <http://link.aps.org/doi/10.1103/PhysRevB.49.11919>.
 - ¹⁵ N. H. Lindner and A. Auerbach, *Physical Review B* **81**, 054512 (2010), URL <http://link.aps.org/doi/10.1103/PhysRevB.81.054512>.
 - ¹⁶ D. Podolsky, A. Auerbach, and D. P. Arovas, *Physical Review B* **84**, 174522 (2011), URL <http://link.aps.org/doi/10.1103/PhysRevB.84.174522>.
 - ¹⁷ K. G. Wilson and M. E. Fisher, *Physical Review Letters* **28**, 240 (1972), URL <http://link.aps.org/doi/10.1103/PhysRevLett.28.240>.
 - ¹⁸ M. Kardar, *Statistical Physics of Fields* (Cambridge University Press, Cambridge, 2007), ISBN 9780511815881, URL <http://ebooks.cambridge.org/ebook.jsf?bid=CB09780511815881>.
 - ¹⁹ I. Affleck and G. F. Wellman, *Physical Review B* **46**, 8934 (1992), URL <http://link.aps.org/doi/10.1103/PhysRevB.46.8934>.
 - ²⁰ J. Oitmaa, Y. Kulik, and O. P. Sushkov, *Physical Review B* **85**, 144431 (2012), URL <http://link.aps.org/doi/10.1103/PhysRevB.85.144431>.
 - ²¹ D. Podolsky and S. Sachdev, *Physical Review B* **86**, 054508 (2012), URL <http://link.aps.org/doi/10.1103/PhysRevB.86.054508>.
 - ²² L. Pollet and N. Prokof'ev, *Physical Review Letters* **109**, 010401 (2012), URL <http://link.aps.org/doi/10.1103/PhysRevLett.109.010401>.
 - ²³ K. Chen, L. Liu, Y. Deng, L. Pollet, and N. Prokof'ev, *Physical Review Letters* **110**, 170403 (2013), URL <http://link.aps.org/doi/10.1103/PhysRevLett.110.170403>.
 - ²⁴ S. Gazit, D. Podolsky, and A. Auerbach, *Physical Review Letters* **110**, 140401 (2013), URL <http://link.aps.org/doi/10.1103/PhysRevLett.110.140401>.
 - ²⁵ S. Gazit, D. Podolsky, A. Auerbach, and D. P. Arovas, *Phys. Rev. B* **88**, 235108 (2013), URL <http://link.aps.org/doi/10.1103/PhysRevB.88.235108>.
 - ²⁶ A. Rançon and N. Dupuis, *Phys. Rev. B* **89**, 180501 (2014), URL <http://link.aps.org/doi/10.1103/PhysRevB.89.180501>.
 - ²⁷ M. J. Bhaseen, J. P. Gauntlett, B. D. Simons, J. Sonner, and T. Wiseman, *Phys. Rev. Lett.* **110**, 015301 (2013), URL <http://link.aps.org/doi/10.1103/PhysRevLett.110.015301>.
 - ²⁸ M. E. Fisher and A. Aharony, *Physical Review B* **10**, 2818 (1974), URL <http://link.aps.org/doi/10.1103/PhysRevB.10.2818>.
 - ²⁹ D. R. Nelson, *Physical Review B* **14**, 1123 (1976), URL <http://link.aps.org/doi/10.1103/PhysRevB.14.1123>.
 - ³⁰ L. Kadanoff, *Physics* **2**, 263 (1966).
 - ³¹ A. Migdal, *Journal of Experimental and Theoretical Physics* **42(3)**, 413 (1975).
 - ³² M. E. Fisher and A. Aharony, *Physical Review Letters* **31**, 1238 (1973), URL <http://link.aps.org/doi/10.1103/PhysRevLett.31.1238>.
 - ³³ S. Sachdev, *Phys. Rev. B* **55**, 142 (1997), URL <http://link.aps.org/doi/10.1103/PhysRevB.55.142>.
 - ³⁴ P. V. Shevchenko, A. W. Sandvik, and O. P. Sushkov, *Phys. Rev. B* **61**, 3475 (2000), URL <http://link.aps.org/doi/10.1103/PhysRevB.61.3475>.
 - ³⁵ Y. Kulik and O. P. Sushkov, *Phys. Rev. B* **84**, 134418 (2011), URL <http://link.aps.org/doi/10.1103/PhysRevB.84.134418>.
 - ³⁶ K. S. D. Beach, arXiv p. 0403055 (2004), URL <http://arxiv.org/abs/cond-mat/0403055v1>.
 - ³⁷ S. Gazit, D. Podolsky, and A. Auerbach, *Phys. Rev. Lett.* **113**, 240601 (2014), URL <http://link.aps.org/doi/10.1103/PhysRevLett.113.240601>.